Research on Chemical Intermediates (2019) 45:5261–5290
https://doi.org/10.1007/s11164-019-03915-z

Preparation of some novel imidazopyridine derivatives of indole as anticancer agents: one-pot multicomponent synthesis, biological evaluation and docking studies

Zohreh Bakherad, et al. *[full author details at the end of the article]*

Received: 7 March 2019 / Accepted: 20 June 2019 / Published online: 13 July 2019
© Springer Nature B.V. 2019

Abstract

A series of novel imidazopyridine derivatives of indole has been synthesized. All the synthesized derivatives were evaluated for their antiproliferative activity against A-549, T-47D, Hep-G2 and MCF-7 human cancer cell lines. The results demonstrated that some of these derivatives exhibited moderate to excellent cytotoxic activities. Compounds **7a** having a cyclohexyl ring substituted to the second amine of imidazopyridyl moiety and phenyl ring of the C-2 indole ring and **7f** with a *para*-methylphenyl ring at the same position exhibited the highest activity against the A-594 cell line with IC_{50} of 11.48 µM and 10.66 µM, respectively. The results indicate that compounds **7a** and **7f** are more cytotoxic towards cancer cell lines compared with etoposide in vitro. In addition, compounds, **7d** and **7j** showed the most potent activity against Hep-G2, equal to etoposide as the standard drug. Also, most of the compounds were inactive against the T-47D and MCF-7 cell lines. The morphological analysis by the acridine orange/ethidium bromide double-staining test and flow cytometry analysis indicated that compounds **7a** and **7f** induced apoptosis in A-549 cells. Furthermore, in silico and in vitro results of the synthesized compounds showed good correlation with each other. Molecular docking results of the compounds of the **7a–k** series with the cyclohexyl ring substituted to the second amine of the imidazopyridyl moiety compared with the **7l–t** members with the t-butyl group at the same position confirmed the effect of the higher lipophilicity on hydrophobic interactions with the studied enzymes. Moreover, all the compounds showed higher affinity to tubulin than topoisomerase IIα enzyme.

Keywords Anticancer agents · Molecular docking · One-pot synthesis · Imidazopyridine ring

Electronic supplementary material The online version of this article (https://doi.org/10.1007/s11164-019-03915-z) contains supplementary material, which is available to authorized users.

Introduction

Cancer is a complex pathological disorder described by a high proliferative index and the spread of abnormal cells from their site of origin [1]. Cancer is the leading origin of death in developed countries and the second leading cause of death in developing countries [2].

Anticancer drug discovery has been strongly focused on the development of drugs intended to act against a specific target with high potency and selectivity. Both topoisomerase II and microtubule are significant anticancer targets, and their respective inhibitors have been extensively used for cancer therapy [3–5]. Microtubules are key components of the cell structure which take part in a varied number of essential cellular functions. In mitosis, the cytoplasmic microtubule is disrupted and reformed as a spindle consisting of large numbers of short microtubules that surround each centrosome [6]. It should be mentioned that this process is significant for the suitable attachment and movement of chromosomes during numerous steps of the mitotic phase. Therefore, inhibition of microtubule formation leads to mitotic arrest and promotes vascular disruption which eventually leads to cell death [7].

Topoisomerases are important cellular enzymes essential for cell proliferation through solving topological problems in the process of DNA replication. Topoisomerase II produces the relaxation of DNA double helices by scissoring and religating the two strands. Because of the critical role of this enzyme for the cell proliferation process, topoisomerase has been one of the main targets in the anticancer drug development field [8]. Topoisomerase II inhibitors and microtubule inhibitors are often used in combination for cancer therapy. Many therapeutic treatments contain vincristine, vinblastine, paclitaxel or docetaxel in combination with doxorubicin or etoposide for the treatment of numerous hematological or solid tumors. These combinations have been reported not only to produce synergistic therapeutic effects but also to reduce nonhematologic toxicities [3]. Heterocyclic compounds are an exceedingly important class of compounds and they have attracted more attention for diverse biological studies [9–11].

Indole analogs comprise a group of the most extensively distributed nitrogen-containing heterocycles in nature having biological significance. The indole ring system is present in various marketed drugs. More often, indoles have been used as drugs for diseases related to the CNS, but in current years researchers have been trying to develop indole-based drugs for combating cancer [12–16]. Perchellet et al. synthesized a collection of novel 6,7-annulated-4-substituted indole compounds to discover a scaffold for anticancer activity. They showed that this class of compounds interacts with tubulin to reduce microtubule assembly [17]. A series of 3-amidoindole derivatives reported by Chen et al. have shown moderate inhibitory activity on tubulin polymerization [18]. In addition, a group of researchers have designed some new 2-phenylindole derivatives as tubulin polymerization inhibitors with low micromolar IC_{50} values which inhibited colchicine binding with a mean value > 70% [19]. Compounds **A** and **B** as the most potent derivatives of 3-amidoindole and 2-phenylindole scaffolds, respectively, are illustrated in Fig. 1.

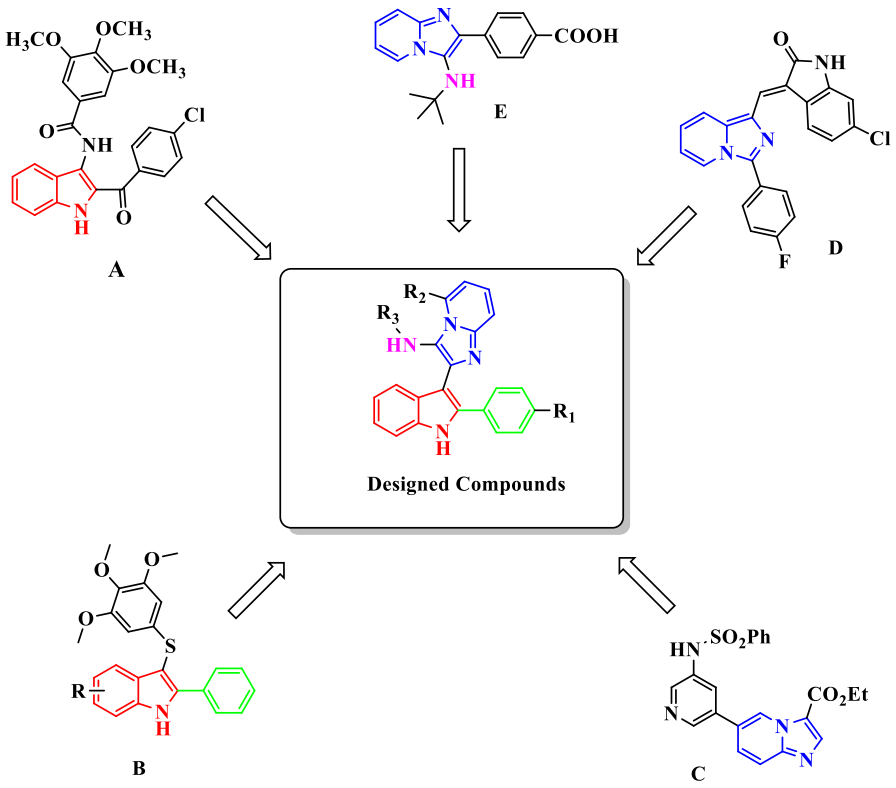

Fig. 1 Structures of indole-based and imidazopyridine-based anticancer agents (**a**–e) and the general structure of the designed compounds

Imidazopyridine is one of the most important fused heterocyclic systems and is known to display a wide range of inhibitory activities for a diverse number of biological targets [20]. This scaffold is also found in some marketed drugs, such as zolpidem and zolimidine [21]. Over the past few years, considerable interest has been devoted to the synthesis and evaluation of the anticancer activity of imidazopyridines [22]. Compounds **C** (ethyl 6-(5-(phenyl sulfonamide) pyridine-3-yl) imidazo[1,2-a]pyridine-3-carboxylate) [23] and **D** ((E)-6-chloro-3-((3-(4-fluorophenyl)imidazo [1,5-a]pyridin-1-yl)methylene)indolin-2-one) [24] with promising anticancer activity have been introduced in such research (Fig. 1). Several derivatives of bicyclic N-fused aminoimidazoles have also been reported by Baviskar et al. They introduced compound **E** (Fig. 1) as a potent topoisomerase IIα catalytic inhibitor which acts via blocking the ATPase binding site of the enzyme without interacting DNA [25].

In the present research, indole and imidazopyridine scaffolds, as effective antiproliferative agents, were subjected to some structural modifications based on a hybridization approach [26]. Hybrid molecules take advantage of affecting different biomolecules, thus they are called multi-target compounds. Three structural motives

were considered in the design of these hybrid molecules. First, the indole moiety for the inhibition of tubulin polymerization, and second, the imidazopyridine structure for its inhibitory activity on the ATPase domain of topoisomerase IIα. The third element which was implemented in the designed structures was a substituted phenyl ring that was proved to be efficient in the anticancer activity of compound **B**. The designed compounds were prepared in the laboratory then evaluated for their in vitro cytotoxic activities. A molecular docking approach against the desired targets was also exploited to confirm the effectiveness of the designed compounds in silico. The general structure of the designed compounds is provided in Fig. 1.

Experimental

Chemistry

All reagents and solvents used in this study are commercially available (from Merck chemical) and were used without further purification. Melting points were determined on a Kofler hot-stage apparatus (Reichert, Vienna, Austria) and uncorrected. Precoated Merck Silica gel 250 μm, F254 TLC aluminium sheets were utilized for thin-layer chromatographic analysis and spots were visualized under UV light at 254 nm. The IR spectra were taken using a Nicolet Magna FT-IR 550 spectrophotometer (potassium bromide disks) and only major peaks are reported in cm^{-1}.

All NMR spectra were recorded on Bruker 500 MHz NMR instruments. Chemical shifts were reported in parts per million (ppm, δ), down-filed from tetramethylsilane coupling constant (*J*) values presented in Hz with spin multicities given as s (singlet), d (double), t (triplet) and m (multiplet). Purification of the compounds was carried out by silica gel column chromatography (230–400 mesh size) with the indicated eluent. Elemental analyses were carried out by a CHN-Rapid Heraeus elemental analyzer. The results of elemental analyses ©, H, N) were within ± 0.4% of the calculated values. For the ease of NMR assignment, all atoms of the scaffold are numbered by simple, prime and double-prime symbols. It should be clarified that this numbering system is different from the IUPAC numbering method. The numbered scaffold is provided in Scheme 1.

General procedure for the synthesis of 2-aryl-1H-indoles (3a–f)

Appropriate amounts of substituted acetophenone **1** (1 mmol) and phenyl hydrazine **2** (1 mmol) were mixed in ethanol (20 mL), and a few drops of glacial acetic acid were added. The solution was heated under reflux at 80 °C for 1–2 h. The solvent was evaporated in vacuo to give a solid that was added to polyphosphoric acid (30 mL), and the mixture was slowly heated to 120 °C and kept at this temperature for a few hours until the reaction was complete (TLC monitoring). The mixture was allowed to cool and then poured into cold water (50 mL). The acidic solution was neutralized by the slow addition of NaOH (1 M), and the solid precipitate of the crude product was collected. Purification by column chromatography (hexane/ethyl

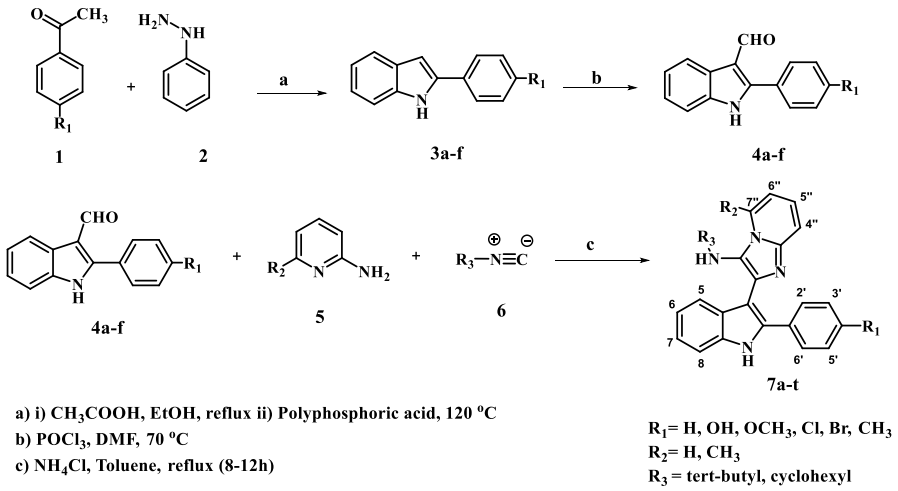

Scheme 1 Synthesis of 2-(2-phenyl-1*H*-indol-3-yl)-imidazo[1,2-a]pyridin-3-amine derivatives (**7a**–**t**)

acetate) gave the substituted 2-aryl indoles **3a**–**t**. Indoles **3a**–**t** were all prepared by a recently reported procedure [27].

General procedure for synthesis of 2-arylindole-3-carbaldehydes (4a–f)

Under nitrogen gas, phosphorous oxychloride (10 mmol) was added dropwise to dry dimethylformamide (DMF) (10 mmol) while cooling in an ice bath, and the reaction mixture was stirred for 1 h. A solution of compound **3** (1 mmol) in DMF (50 ml) was added dropwise to the mixture with continuous stirring, which was then heated to 70 °C. The mixture was poured onto ice cold water (200 mL), naturalized with 40% NaOH, and extracted with chloroform. The chloroform extract was washed with water and dried over Na_2SO_4. The solvent was removed under vacuum. The residue was crystalized from an ethanol/water mixed solvent system [27].

2-Phenyl-1H-indole-3-carbaldehyde (4a)

Cream powder; Mp: 249–250 °C; Yield: 89%; IR (KBr, cm^{-1}): 3144 (NH), 2858 (H–CO), 1625 (C=O), 1455 (C=C). ^{1}H NMR (500 MHz, DMSO-d_6) (δ, ppm): 7.24 (t, J = 7.9 Hz, 1H, H_6), 7.29 (t, J = 7.9 Hz, 1H, H_7), 7.51 (d, J = 7.9 Hz, 1H, H_8), 7.56–7.62 (m, 3H, $H_{3',5',4'}$), 7.78 (d, J = 9.3 Hz, 2H, $H_{2',6'}$), 8.21 (d, J = 7.9 Hz, 1H, H_5), 9.96 (s, 1H, CHO), 12.40 (s, 1H, NH-indole). ^{13}C NMR (125 MHz, DMSO-d_6) (***δ***, ppm): 112.1, 113.5, 121.2, 122.5, 123.7, 125.8, 128.9, 129.2, 129.8, 130.1, 135.9, 149.1, 185.5. Anal. Calcd. for $C_{15}H_{11}NO$: C, 81.43; H, 5.01; N, 6.33. Found: C, 81.53; H, 4.85; N, 6.45.

2-(4-Hydroxyphenyl)-1H-indole-3-carbaldehyde (4b)

Cream powder; Mp: 225–227 °C; Yield: 86%; IR (KBr, cm^{-1}): 3151 (OH), 3074 (NH), 2862 (H–CO), 1619 (C=O), 1455 (C=C), 1177 (C–O) ^{1}H NMR (500 MHz, DMSO-d_6) (δ, ppm): 6.97 (d, $J=7.6$ Hz, 2H, $H_{3',5'}$), 7.19–7.26 (m, 2H, $H_{6,7}$), 7.45 (d, $J=7.5$ Hz, 1H, H_8), 7.60 (d, $J=7.6$ Hz, 2H, $H_{2',6'}$), 8.17 (d, $J=7.5$ Hz, 1H, H_5), 9.92 (s, 1H, CHO), 10.04 (s, 1H, OH), 12.20 (s, 1H, NH-indole). ^{13}C NMR (125 MHZ, DMSO-d_6) (δ, ppm): 111.6, 112.7, 115.8, 120.4, 120.9, 122.2, 123.3, 125.9, 131.2, 135.8, 149.8, 159.1, 185.5. Anal. Calcd. for $C_{15}H_{11}NO_2$: C, 75.94; H, 4.67; N, 5.93. Found: C, 76.04; H, 4.71; N, 5.72.

2-(4-Methoxyphenyl)-1H-indole-3-carbaldehyde (4c)

Cream powder, Mp: 207–209 °C; Yield: 90%. IR (KBr, cm^{-1}): 3147 (NH), 2837 (H–CO), 1621 (C=O), 1454 (C=C), 1179 (C–O). ^{1}H NMR (500 MHz, DMSO-d_6) (δ, ppm): 3.87 (s, 3H, OCH_3), 7.16 (d, $J=8.7$ Hz, 2H, $H_{3',5'}$), 7.20–7.28 (m, 2H, $H_{6,7}$), 7.47 (d, $J=7.6$ Hz, 1H, H_8), 7.72 (d, $J=8.7$ Hz, 2H, $H_{2',6'}$), 8.18 (d, $J=7.6$ Hz, 1H, H_5), 9.94 (s, 1H, CHO), 12.28 (s, 1H, NH-indole). ^{13}C NMR (125 MHZ, DMSO-d_6) (δ, ppm): 55.8, 111.8, 113.2, 114.7, 120.9, 122.0, 122.4, 123.7, 125.9, 131.4, 135.9, 149.3, 160.6, 185.4. Anal. Calcd. for $C_{16}H_{13}NO_2$: C, 76.48; H, 5.21; N, 5.57. Found: C, 76.60; H, 5.29; N, 5.48.

2-(4-Chlorophenyl)-1H-indole-3-carbaldehyde (4d)

Cream powder, Mp > 250 °C; Yield: 88%. IR (KBr, cm^{-1}): 3168 (NH), 2866 (H–CO), 1625 (C=O), 1450 (C=C). ^{1}H NMR (500 MHz, DMSO-d_6) (δ, ppm): 7.25 (t, $J=7.6$ Hz, 1H, H_6), 7.30 (t, $J=7.6$ Hz, 1H, H_7), 7.51 (d, $J=7.6$ Hz, 1H, H_8), 7.74 (d, $J=8.1$ Hz, 2H, $H_{3',5'}$), 7.80 (d, $J=8.1$ Hz, 2H, $H_{2',6'}$), 8.21 (d, $J=7.6$ Hz, 1H, H_5), 9.95 (s, 1H, CHO), 12.46 (s, 1H, NH-indole). ^{13}C NMR (125 MHZ, DMSO-d_6) (δ, ppm): 112.1, 113.6, 121.1, 122.6, 123.5, 123.9, 125.8, 129.0, 131.8, 132.0, 135.9, 147.4, 185.4. Anal. Calcd. for $C_{15}H_{10}ClNO$: C, 70.46; H, 3.94; N, 5.48. Found: C, 70.69; H, 3.85; N, 5.51.

2-(4-Bromophenyl)-1H-indole-3-carbaldehyde (4e)

Cream powder, Mp > 250 °C; Yield: 92%. IR (KBr, cm^{-1}): 3167 (NH), 2840 (H–CO), 1623 (C=O), 1452 (C=C). ^{1}H NMR (500 MHz, DMSO-d_6) (δ, ppm): 7.25 (t, $J=7.6$ Hz, 1H, H_6), 7.30 (t, $J=7.6$ Hz, 1H, H_7), 7.51 (d, $J=7.6$ Hz, 1H, H_8), 7.74 (d, $J=8.3$ Hz, 2H, $H_{3',5'}$), 7.80 (d, $J=8.3$ Hz, 2H, $H_{2',6'}$), 8.20 (d, $J=7.6$ Hz, 1H, H_5), 9.95 (s, 1H, CHO), 12.47 (s, 1H, NH-indole). ^{13}C NMR (125 MHZ, DMSO-d_6) (δ, ppm): 112.1, 113.6, 121.1, 122.6, 123.5, 123.9, 125.5,

128.8, 131.9, 132.0, 136.2, 147.4, 185.2. Anal. Calcd. for $C_{15}H_{10}BrNO$: C, 60.02; H, 3.36; N, 4.67. Found: C, 60.21; H, 3.48; N, 4.60.

2-p-Tolyl-1H-indole-3-carbaldehyde (4f)

Cream powder, Mp: 239–241 °C, Yield: 88%. IR (KBr, cm^{-1}): 3213 (NH), 2863 (H–CO), 1625 (C=O), 1452 (C=C). ^{1}H NMR (500 MHz, DMSO-d_6) (δ, ppm): 2.41 (s, 3H, CH_3), 7.23 (t, $J=7.5$ Hz, 1H, H_6), 7.28 (t, $J=7.5$ Hz, 1H, H_7), 7.41 (d, $J=7.9$ Hz, 2H, $H_{3',5'}$), 7.49 (d, $J=7.5$ Hz, 1H, H_8), 7.67 (d, $J=7.9$ Hz, 2H, $H_{2',6'}$), 8.19 (d, $J=7.5$ Hz, 1H, H_5), 9.95 (s, 1H, CHO), 12.34 (s, 1H, NH-indole). ^{13}C NMR (125 MHZ, DMSO-d_6) (δ, ppm): 21.0, 112.0, 113.3, 121.1, 122.4, 123.6, 125.8, 126.9, 129.6, 129.9, 135.9, 139.7, 149.1, 184.9. Anal. Calcd. for $C_{16}H_{13}NO$: C, 81.68; H, 5.57; N, 5.97. Found: C, 81.78; H, 5.48; N, 5.79.

General procedure for synthesis of 2-(2-phenyl-1H-indol-3-yl)H-imidazo[1,2-a] pyridin-3-amine (7a–t)

A mixture of 2-arylindole-3-carbaldehydes (**4a**–**f**) (1 mmol), diverse pyridine 2-amines (**5**) (1 mmol), varied isocyanides (**6**) (1.2 mmol) and ammonium chloride (1 mmol) were suspended in 15 mL of toluene. The reaction mixture was heated and stirred under reflux until the end of the reaction. After the completion of the reaction, the mixture was cooled to room temperature and then concentrated under vacuum and purified by ethyl acetate/n-hexane [30].

N-cyclohexyl-2-(2-phenyl-1H-indol-3-yl)H-imidazo[1,2-a]pyridin-3-amine (7a)

White powder, Mp > 250 °C; Yield: 75%, IR (KBr, cm^{-1}): 3359, 3310 (N–H stretching), 3058 (aromatic C–H stretching), 2926 (aliphatic C–H stretching), 1628 (C=N), 1582 (C=C), 1452 (CH_2 bending), 1230 (C–N); ^{1}H NMR (500 MHz, DMSO-d6) (δ, ppm): 0.74–0.78 (m, 4H, cyclohexyl), 0.89–0.91 (m, 1H, cyclohexyl), 1.29–1.31 (m, 5H, cyclohexyl), 1.98 (m, 1H, NH), 3.08–3.16 (m, 1H, CH), 6.86 (t, $J=7.3$ Hz, 1H, $H_{6''}$), 7.01 (t, $J=7.3$ Hz, 1H, $H_{5''}$), 7.14 (t, $J=7.6$ Hz, 2H, $H_{6,7}$), 7.30–7.32 (m, 1H, $H_{4'}$), 7.40 (t, $J=7.3$ Hz, 2H, $H_{3',5'}$), 7.44 (d, $J=7.3$ Hz, 1H, H_8), 7.50 (d, $J=7.3$ Hz, 1H, $H_{4''}$), 7.55 (d, $J=7.3$ Hz, 2H, $H_{2',6'}$), 7.62 (d, $J=7.6$ Hz, 1H, H_5), 8.19 (d, $J=7.3$, 1H, $H_{6''}$), 11.53 (s, 1H, NH-indole). ^{13}C NMR (125 MHZ, DMSO-d6) (δ, ppm): 23.8, 23.3, 32.7, 54.52, 106.7, 111.0, 111.2, 116.4, 116.5, 119.2, 120.2, 121.8, 122.5, 122.7, 122.9, 125.8, 127.1, 127.5, 128.8, 129.1, 133.2, 136.0, 140.4. MS (ESI) *m/z*: 407 (MH^+). Anal. Calcd for $C_{27}H_{26}N_4$: C, 79.77; H, 6.45; N, 13.78; Found C, 79.91; H, 6.35; N, 13.90.

4-(3-(3-(cyclohexylamino)H-imidazo[1,2-a]pyridin-2-yl)-1H-indol-2-yl)phenol (7b)

Pale yellow powder, Mp: 177–180 °C; Yield: 82%. IR (KBr, cm^{-1}): 3405 (O–H), 3343 (N–H stretching), 3057 (aromatic C–H stretching), 2927 (aliphatic C–H stretching), 1634 (C=N), 1584 (C=C), 1450 (CH_2 bending), 1238 (C–N), 1176

(C–O). ^{1}H NMR (500 MHz, DMSO-d6) (***δ***, ppm): 0.72–0.83 (m, 4H, cyclohexyl), 0.90–0.94 (m, 1H, cyclohexyl), 1.26–1.34 (m, 5H, cyclohexyl), 2.20 (m, 1H, NH), 2.95–2.96 (m, 1H, CH), 6.79 (d, $J=8.5$ Hz, 2H, $H_{3',5'}$), 6.84 (t, $J=7.4$ Hz, 1H, $H_{6''}$), 6.98 (t, $J=7.4$ Hz, 1H, $H_{5''}$), 7.08–7.14 (m, 2H, $H_{6,7}$), 7.35 (d, $J=8.5$ Hz, 2H, $H_{2',6'}$), 7.39 (d, $J=7.9$ Hz, 1H, H_8), 7.49 (d, $J=7.4$ Hz, 1H, $H_{4''}$), 7.64 (d, $J=7.9$ Hz, 1H, H_5), 8.16 (d, $J=7.4$ Hz, 1H, $H_{7''}$), 9.67 (s, 1H, OH), 11.36 (s, 1H, NH-indole). ^{13}C NMR (125 MHZ, DMSO-d6) (***δ***, ppm): 22.8, 24.4, 31.3, 55.6, 106.4, 110.7, 111.0, 114.8, 115.2, 117.5, 121.2, 122.1, 124.5, 126.0, 126.8, 130.0, 130.6, 134.4, 135.5, 137.6, 140.9, 143.2, 156.5. MS (ESI) *m/z*: 423 (MH^+). Anal. Calcd for $C_{27}H_{26}N_4O$: C, 76.75; H, 6.20; N, 13.26; Found C, 76.51; H, 6.10; N, 13.37.

N-cyclohexyl-2-(2-(4-methoxyphenyl)-1H-indol-3-yl)H-imidazo[1,2-a] pyridin-3-amine (**7c**)

Cream powder, Mp > 250 °C; Yield: 79%. IR (KBr, cm^{-1}): 3409 (N–H stretching), 3063 (aromatic C–H stretching), 2929 (aliphatic C–H stretching),1653 (C=N), 1611 (C=C), 1454 (CH_2 bending), 1250 (C–N), 1178 (C–O). ^{1}H NMR (500 MHz, DMSO-d6) (δ, ppm): 0.78–0.79 (m, 4H, cyclohexyl), 0.90–0.92 (m, 1H, cyclohexyl), 1.27–1.33 (m, 5H, cyclohexyl), 1.98 (m, 1H, NH), 3.19–3.20 (m, 1H, CH), 6.86 (t, $J=7.4$ Hz, 1H, $H_{6''}$), 6.97–7.00 (m, 3H, $H_{3',5',5''}$), 7.10–7.16 (m, 2H, $H_{6,7}$), 7.41 (d, $J=7.9$ Hz, 1H, H_8), 7.48–7.50 (m, 3H, $H_{4'',2',6'}$), 7.56 (d, $J=7.9$ Hz, 1H, H_5), 8.19 (d, $J=7.4$ Hz, 1H, $H_{7''}$), 11.42 (s, 1H, NH-indole). ^{13}C NMR (125 MHZ, DMSO-d6) (δ, ppm): 23.8, 25.2, 32.6, 54.5, 55.3, 110.8, 114.4, 116.6, 118.2, 119.6, 121.8, 123.1, 125.6, 126.5, 128.5, 129.5, 129.6, 131.8, 132.7, 133.4, 134.6, 135.1, 140.0, 158.8. MS (ESI) *m/z*: 437 (MH^+). Anal. Calcd for $C_{28}H_{28}N_4O$: C, 77.04; H, 6.46; N, 12.83; Found C, 77.15; H, 6.24; N, 12.71.

2-(2-(4-chlorophenyl)-1H-indol-3-yl)-N-cyclohexylH-imidazo[1,2-a]pyridin-3-amine (**7d**)

Dark cream powder, Mp > 250 °C; Yield: 78%, IR (KBr, cm^{-1}): 3448 (N–H stretching), 3059 (aromatic C–H stretching), 2928 (aliphatic C–H stretching), 1628 (C=N), 1581 (C=C), 1451 (CH_2 bending), 1230 (C–N). ^{1}H NMR (500 MHz, DMSO-d6) (δ, ppm): 0.73–0.81 (m, 4H, cyclohexyl), 0.89–0.91 (m, 1H, cyclohexyl), 1.31–1.33 (m, 5H, cyclohexyl), 1.99 (broad, 1H, NH), 3.48–3.50 (m, 1H, CH), 6.87 (t, $J=6.8$ Hz, 1H, $H_{6''}$), 7.00 (t, $J=6.8$ Hz, 1H, $H_{5''}$), 7.12–7.17 (m, 2H, $H_{6,7}$), 7.44 (d, $J=8.0$ Hz, 2H, $H_{3',5'}$), 7.49–7.54 (m, 3H, $H_{5,8,4''}$), 7.57 (d, $J=8.0$ Hz, 2H, $H_{2',6'}$), 8.22 (d, $J=6.8$ Hz, 1H, $H_{7''}$), 11.60 (s, 1H, NH-indole). ^{13}C NMR (125 MHZ, DMSO-d6) (δ, ppm): 23.9, 25.3, 32.8, 54.4, 107.3, 111.0, 116.5, 116.6, 119.4, 120.0, 120.1, 120.6, 122.1, 122.5, 122.8, 123.0, 126.2, 128.7, 129.2, 132.0, 133.8, 136.1, 140.4. MS (ESI) *m/z*: 441 (MH^+). Anal. Calcd for $C_{27}H_{25}ClN_4$: C, 73.54; H, 5.71; N, 12.71; Found C, 73.41; H, 5.90; N, 12.89.

2-(2-(4-bromophenyl)-1H-indol-3-yl)-N-cyclohexylH-imidazo[1,2-a]pyridin-3-amine (**7e**)

Cream to yellow powder, Mp = 242–244 °C; Yield: 76%, IR (KBr, cm^{-1}): 3449 (N–H stretching), 3061 (aromatic C–H stretching), 2928 (aliphatic C–H stretching),1629 (C=N), 1581 (C=C), 1451 (CH_2 bending), 1229 (C–N). ^{1}H NMR (500 MHz, DMSO-d6) (δ, ppm): 0.64–0.66 (m, 4H, cyclohexyl), 0.90–1.00 (m, 1H, cyclohexyl), 1.27–1.38 (m, 5H, cyclohexyl), 2.06 (broad, 1H, NH), 3.13–3.17 (m, 1H, CH), 7.10 (t, J = 6.8 Hz, 1H, $H_{6''}$), 7.24 (t, J = 6.8 Hz, 1H, $H_{5''}$), 7.47–7.55 (m, 5H, $H_{5,6,7,8,4''}$), 7.62 (d, J = 7.9 Hz, 2H, $H_{3',5'}$), 7.82–7.86 (m, 2H, $H_{2',6'}$), 8.77 (d, J = 6.8 Hz, 1H, $H_{7''}$), 12.28 (s, 1H, NH-indole). ^{13}C NMR (125 MHZ, DMSO-d6) (δ, ppm): 24.0, 24.8, 32.7, 53.7, 111.8, 111.9, 119.0, 1119.1, 120.4, 121.6, 122.9, 123.0, 124.9, 125.0, 128.2, 128.6, 129.2, 130.5, 131.2, 131.9, 135.9, 136.1, 136.4. MS (ESI) *m/z*: 485 (MH^+). Anal. Calcd for $C_{27}H_{25}BrN_4$: C, 66.81; H, 5.19; N, 11.54 Found C, 66.61; H, 5.05; N, 11.64.

N-cyclohexyl-2-(2-p-tolyl-1H-indol-3-yl)H-imidazo[1,2-a]pyridin-3-amine (**7f**)

White powder, Mp > 250 °C; Yield: 72%, IR (KBr, cm^{-1}): 3351, 3131 (N–H stretching), 3063 (aromatic C–H stretching), 2927 (aliphatic C–H stretching),1624 (C=N), 1583 (C=C), 1453 (CH_2 bending), 1225 (C–N). ^{1}H NMR (500 MHz, DMSO-d6) (δ, ppm): 0.76–0.78 (m, 4H, cyclohexyl), 0.90–0.91 (m, 1H, cyclohexyl), 1.26–1.31 (m, 5H, cyclohexyl), 1.99 (broad, 1H, NH), 2.30 (s, 3H, CH_3), 3.07–3.08 (m, 1H, CH), 6.85 (t, J = 7.5 Hz, 1H, $H_{6''}$), 7.00 (t, J = 7.5 Hz, 1H, $H_{5''}$), 7.12–7.15 (m, 2H, $H_{6,7}$), 7.21 (d, J = 8.0 Hz, 2H, $H_{3',5'}$), 7.41–7.44 (m, 3H, $H_{2',6',8}$), 7.49 (d, J = 7.5 Hz, 1H, $H_{4''}$), 7.60 (d, J = 8.0 Hz, 1H, H_5), 8.18 (d, J = 7.5 Hz, 1H, $H_{7''}$), 11.47 (s, 1H, NH-indole). ^{13}C NMR (125 MHZ, DMSO-d6) (δ, ppm): 24.4, 25.2, 29.8, 32.6, 55.1, 114.21, 117.6, 119.4, 121,7, 122.5, 124.8, 125.5, 126.5, 127.0, 127.5, 128.3, 128.6, 129.3, 130.9, 135.1, 135.9, 137.0, 139.0, 141.2. MS (ESI) *m/z*: 421 (MH^+). Anal. Calcd for $C_{28}H_{28}N_4$: C, 79.97; H, 6.71; N, 13.32 Found C, 80.10; H, 6.90; N, 13.15.

4-(3-(3-(cyclohexylamino)-5-methylH-imidazo[1,2-a]pyridin-2-yl)-1H-indol-2-yl) phenol (**7g**)

Cream powder, Mp: 228–230 °C; Yield: 75%, IR (KBr, cm^{-1}): 3349 (O–H), 3338 (N–H stretching), 3059 (aromatic C–H stretching), 2926 (aliphatic C–H stretching),1612 (C=N), 1575 (C=C), 1450 (CH_2 bending), 1228 (C–N), 1178 (C–O). ^{1}H NMR (500 MHz, DMSO-d6) (δ, ppm): 0.61–0.79 (m, 6H, cyclohexyl), 1.24–1.25 (m, 4H, cyclohexyl), 1.98 (s, 1H, NH), 2.60–2.65 (m, 1H, CH), 2.83 (s, 3H, CH_3), 6.51 (d, J = 7.0 Hz, 1H, $H_{6''}$), 6.80 (d, J = 8.0 Hz, 2H, $H_{3',5'}$), 6.97–7.03 (m, 2H, $H_{6,7}$), 7.09 (t, J = 7.0 Hz, 1H, $H_{5''}$), 7.33 (d, J = 8.4 Hz, 1H, H_8), 7.38–7.41 (m, 3H, $H_{2',6',4''}$), 7.63 (d, J = 8.4 Hz, 1H, H_5), 9.67 (s, 1H, OH), 11.32 (s, 1H, NH-indole). ^{13}C NMR (125 MHZ, DMSO-d6) (δ, ppm): 19.4, 23.8, 25.2, 32.1, 56.9, 112.5, 114.8, 114.9, 115.7, 118.9, 119.7, 121.2, 122.9, 124.0, 126.9, 128.4, 128.5, 129.1, 134.5, 135.5, 135.9, 136.1, 142.3, 157.1. MS (ESI) *m/z*: 437 (MH^+). Anal. Calcd for $C_{28}H_{28}N_4O$: C, 77.04; H, 6.46; N, 12.83; Found C, 76.85; H, 6.65; N, 12.97.

N-cyclohexyl-2-(2-(4-methoxyphenyl)-1H-indol-3-yl)-5-methylH-imidazo[1,2-a] pyridin-3-amine (7h)

Light cream powder, Mp: 203–205 °C; Yield: 69%, IR (KBr, cm^{-1}): 3343, 3130 (N–H stretching), 3057 (aromatic C–H stretching), 2926 (aliphatic C–H stretching), 1606 (C=N), 1543 (C=C), 1452 (CH_2 bending), 1242 (C–N), 1179 (C–O). ^{1}H NMR (500 MHz, DMSO-d6) (δ, ppm): 0.63–0.85 (m, 6H, cyclohexyl), 1.24–1.26 (m, 4H, cyclohexyl), 1.99 (s, 1H, NH), 2.78–2.79 (m, 1H, CH), 2.85 (s, 3H, CH_3), 3.76 (s, 3H, CH_3), 6.53 (d, $J=7.3$ Hz, 1H, $H_{6''}$), 6.97–7.04 (m, 3H, $H_{6,7,3',5'}$), 7.12 (t, $J=7.3$ Hz, 1H, $H_{5''}$), 7.34 (d, $J=9.0$ Hz, 1H, H_8), 7.41 (d, $J=7.3$ Hz, 1H, $H_{4''}$), 7.53–7.58 (m, 4H, $H_{5,2',6'}$), 11.42 (s, 1H, NH-indole). ^{13}C NMR (125 MHZ, DMSO-d6) (δ, ppm): 19.6, 23.5, 25.2, 32.1, 55.0, 56.41, 110.9, 112.5, 114.2, 114.9, 119.2, 119.7, 121.3, 123.0, 125.3, 127.2, 128.2, 128.5, 129.1, 134.9, 136.1, 140.3, 142.3, 146.3, 158.8. MS (ESI) *m/z*: 451 (MH^+). Anal. Calcd for $C_{29}H_{30}N_4O$: C, 77.30; H, 6.71; N, 12.43; Found C, 77.57; H, 6.51; N, 12.53.

2-(2-(4-chlorophenyl)-1H-indol-3-yl)-N-cyclohexyl-5-methylH-imidazo[1,2-a] pyridin-3-amine (7i)

Light green, Mp: 250 °C; Yield: 79%, IR (KBr, cm^{-1}): 3143 (N–H stretching), 3044 (aromatic C–H stretching), 2930 (aliphatic C–H stretching),1653 (C=N), 1543 (C=C), 1446 (CH_2 bending), 1262 (C–N). ^{1}H NMR (500 MHz, DMSO-d6) (δ, ppm): 0.68–0.74 (m, 4H, cyclohexyl), 0.85–0.87 (m, 1H, cyclohexyl), 1.24–1.25 (m, 5H, cyclohexyl), 1.99 (s, 1H, NH), 2.91 (s, 3H, CH_3), 3.05–3.06 (m, 1H, CH), 6.56 (d, $J=6.8$ Hz, 1H, $H_{6''}$), 7.06–7.12 (m, 2H, $H_{6,7}$), 7.20 (t, $J=6.8$ Hz, 1H, $H_{5''}$), 7.35 (d, $J=9.1$ Hz, 1H, H_8), 7.47–7.51 (m, 3H, $H_{4'',3',5'}$), 7.57 (d, $J=9.1$ Hz, H_5), 7.64 (d, $J=8.5$ Hz, 2H, $H_{2',6'}$), 11.63 (s, 1H, NH-indole). ^{13}C NMR (125 MHZ, DMSO-d6) (δ, ppm): 19.8, 23.3, 25.05, 32.1, 55.1, 109.9, 112.0, 114.8, 116.2, 117.7, 119.4, 120.4, 122.2, 122.9, 124.6, 128.0, 129.0, 129.2, 130.1, 133, 136.0, 138.3, 139.8, 141.1. MS (ESI) *m/z*: 455 (MH^+). Anal. Calcd for $C_{28}H_{27}ClN_4$: C, 73.91; H, 5.98; N, 12.31 Found C, 73.65; H, 5.80; N, 12.54.

2-(2-(4-bromophenyl)-1H-indol-3-yl)-N-cyclohexyl-5-methylH-imidazo[1,2-a] pyridin-3-amine (7j)

Yellow powder, Mp: 230–233 °C; Yield: 81%, IR (KBr, cm^{-1}): 3146 (N–H stretching), 3059 (aromatic C–H stretching), 2922 (aliphatic C–H stretching), 1651 (C=N), 1537 (C=C), 1450 (CH_2 bending), 1230 (C–N). ^{1}H NMR (500 MHz, DMSO-d6) (δ, ppm): 0.66–0.74 (m, 5H, cyclohexyl), 1.24–1.25 (m, 5H, cyclohexyl), 1.98 (s, 1H, NH), 2.88 (s, 3H, CH_3), 3.03–3.04 (m, 1H, CH), 6.54 (d, $J=7.0$ Hz, 1H, $H_{6''}$), 7.00–7.05 (m, 2H, $H_{6,7}$), 7.16 (t, $J=7.0$ Hz, 1H, $H_{5''}$), 7.33 (d, $J=8.4$ Hz, 1H, H_8), 7.43–7.47 (m, 3H, $H_{4'',3',5'}$), 7.55 (d, $J=8.4$ Hz, H_5), 7.64 (d, $J=8.4$ Hz, 2H, $H_{2',6'}$), 11.60 (s, 1H, NH-indole). ^{13}C NMR (125 MHZ, DMSO-d6) (δ, ppm): 20.1, 23.2, 24.7, 31.9, 54.9, 109.1, 110.7, 112.8, 116.4, 117.2, 119.4, 120.4, 121.5, 122.1,

124.7, 125.9, 127.6, 128.9, 129.6, 131.6, 133.3, 136.8, 137.6, 140.8. MS (ESI) *m/z*: 499 (MH^+). Anal. Calcd for $C_{30}H_{31}BrN_4$: C, 68.31; H, 5.92; N, 10.62 Found C, 68.15; H, 6.10; N, 10.41.

N-cyclohexyl-5-methyl-2-(2-p-tolyl-1H-indol-3-yl)H-imidazo[1,2-a]pyridin-3-amine (7k)

White powder, Mp > 250 °C; Yield 71%, IR (KBr, cm^{-1}): 3350, 3131 (N–H stretching), 3027 (aromatic C–H stretching), 2927 (aliphatic C–H stretching), 1453 ((CH_2 bending), 1642 (C=N), 1583 (C=C), 1227 (C–N). ^{1}H NMR (500 MHz, DMSO-d6) (δ, ppm): 0.64 (m, 6H, cyclohexyl), 1.24–1.25 (m, 4H, cyclohexyl), 1.99 (s, 1H, NH), 2.31 (s, 3H, CH3), 2.79 (broad, 1H, CH), 2.86 (s, 3H, CH_3), 6.54 (d, J = 6.4 Hz, 1H, $H_{6''}$), 7.00–7.06 (m, 2H, $H_{6,7}$), 7.13 (t, J = 6.4 Hz, 1H, $H_{5''}$), 7.22 (d, J = 6.0, 2H, $H_{3',5'}$), 7.33 (d, J = 7.5 Hz, 1H, H_8), 7.43 (d, J = 6.4 Hz, $H_{4''}$), 7.50 (d, J = 6.0 Hz, 2H, $H_{2',6'}$), 7.60 (d, J = 7.5 Hz, H_5), 11.67 (s, 1H, NH-indole). ^{13}C NMR (125 MHZ, DMSO-d6) (δ, ppm): 22.9, 23.5, 25.1, 30.4, 32.2, 56.0, 114.6, 115.2, 119.2, 120.4, 120.8, 122.4, 123.2, 124.0, 125.6, 126.5, 127.4, 128.2, 131.2, 133.6, 134.6, 136.0, 137.8, 138.3, 142.1. MS (ESI) *m/z*: 435 (MH^+). Anal. Calcd for $C_{29}H_{30}N_4$ C, 80.15; H, 6.96; N, 12.89 Found C, 80.35; H, 7.25; N, 12.63.

N-tert-butyl-2-(2-phenyl-1H-indol-3-yl)H-imidazo[1,2-a]pyridin-3-amine (7l)

Creamish White powder, Mp > 250 °C; Yield 79%, IR (KBr, cm^{-1}): 3432, 3339 (N–H stretching), 3061 (aromatic C–H stretching), 2963 (aliphatic C–H stretching), 1629 (C=N), 1584 (C=C), 1454 (CH_2 bending), 1216 (C–N). ^{1}H NMR (500 MHz, DMSO-d6) (δ, ppm): 0.64 (s, 9H, t-butyl), 1.98 (s, 1H, NH), 6.84 (d, J = 6.7 Hz, 1H, $H_{6''}$), 7.03 (t, J = 6.7 Hz, 1H, $H_{5''}$), 7.13–7.19 (m, 2H, $H_{6,7}$), 7.35 (t, J = 6.7 Hz, 1H, H_8), 7.42–7.45 (m, 3H, $H_{3',5',8}$), 7.50–7.53 (m, 3H, $H_{2',6',4''}$), 7.77 (d, J = 7.6 Hz, 1H, H_5), 8.28 (d, J = 6.7 Hz, 1H, $H_{7''}$), 11.52 (s, 1H, NH-indole). ^{13}C NMR (125 MHZ, DMSO-d6) (δ, ppm): 29.0, 55.08, 107.5, 110.8, 111.2, 116.4, 116.5, 119.3, 120.5, 123.2, 123.5, 123.7, 127.1, 127.2, 127.7, 128.8, 129.1, 133.4, 134.9, 136.4, 141.5. MS (ESI) *m/z*: 381 (MH^+). Anal. Calcd for $C_{25}H_{24}N_4$ C, 78.92; H, 6.36; N, 14.73 Found C, 79.14; H, 6.49; N, 14.69.

4-(3-(3-(tert-butylamino)H-imidazo[1,2-a]pyridin-2-yl)-1H-indol-2-yl)phenol (7m)

White powder, Mp < 250 °C; Yield 81%, IR (KBr, cm^{-1}): 3449, 3339 (N–H stretching), 3060 (aromatic C–H stretching), 2923 (aliphatic C–H stretching), 1606 (C=N), 1544 (C=C), 1448 (CH_2 bending), 1219 (C–N), 1180 (C–O). ^{1}H NMR (500 MHz, DMSO-d6) (δ, ppm): 0.64 (s, 9H, t-butyl), 1.98 (s, 1H, NH), 6.82–6.84 (m, 3H, $H_{3',5',6''}$), 7.00 (t, J = 7.9 Hz, 1H, $H_{5''}$), 7.10 (t, J = 7.7 Hz, 1H, H_6), 7.16 (t, J = 7.7 Hz, 1H, H_7), 7.30 (d, 2H, $H_{2',6'}$), 7.38 (d, J = 7.7 Hz, 1H, H_8), 7.51 (d, J = 7.9 Hz, 1H, $H_{4''}$), 7.76 (d, J = 7.7 Hz, 1H, H_5), 8.27 (d, J = 7.9 Hz, 1H, $H_{7''}$), 11.34 (s, 1H, NH-indole). ^{13}C NMR (125 MHZ, DMSO-d6) (δ, ppm): 28.9, 54.8, 106.3, 110.6, 115.7, 116.3, 116.4, 119.0, 120.1, 121.3, 123.0, 123.5, 124.2, 128.5, 128.7, 128.9, 135.3,

135.5, 136.1, 141.4, 157.2. MS (ESI) *m/z*: 397 (MH^+). Anal. Calcd for $C_{25}H_{24}N_4O$ C, 75.73; H, 6.10; N, 14.13; Found C, 75.98; H, 5.97; N, 13.89.

N-tert-butyl-2-(2-(4-methoxyphenyl)-1H-indol-3-yl)H-imidazo[1,2-a]pyridin-3-amine (7n)

Cream powder, Mp > 250 °C; Yield 75%, IR (KBr, cm^{-1}): 3338 (N–H stretching), 3061 (aromatic C–H stretching), 2965 (aliphatic C–H stretching), 1615 (C=N), 1539 (C=C), 1454 (CH_2 bending), 1248 (C–N), 1180 (C–O). ^{1}H NMR (500 MHz, DMSO-d6) (δ, ppm): 0.65 (s, 9H, t-butyl), 1.99 (s, 1H, NH), 3.78 (s, 3H, CH_3), 6.84 (t, J = 7.3 Hz, 1H, $H_{6''}$), 7.01–7.03 (m, 3H, $H_{3',5',5''}$), 7.12 (t, J = 7.6 Hz, 1H, H_6), 7.17 (t, J = 7.6 Hz, 1H, H_7), 7.40 (d, J = 7.6 Hz, 1H, H_8), 7.44 (d, J = 8.1 Hz, 2H, $H_{2',6'}$), 7.51 (d, J = 7.3 Hz, 1H, $H_{4''}$), 7.71 (d, J = 7.6 Hz, 1H, H_5), 8.29 (d, J = 7.3 Hz, 1H, $H_{7''}$), 11.41 (s, 1H, NH-indole). ^{13}C NMR (125 MHZ, DMSO-d6) (δ, ppm): 28.9, 55.2, 54.8, 106.7, 110.4, 111.0, 114.6, 116.3, 118.8, 119.9, 121.4, 122.8, 123.5, 123.7, 125.5,128.4, 128.6, 128.9, 135.0, 136.3, 141.5, 158.7. MS (ESI) *m/z*: 411 (MH^+); Anal. Calcd for $C_{26}H_{26}N_4O$ C, 76.07; H, 6.38; N, 13.65; Found C, 76.23, 6.49, 13.51.

N-tert-butyl-2-(2-(4-chlorophenyl)-1H-indol-3-yl)H-imidazo[1,2-a]pyridin-3-amine (7o)

Cream powder, Mp > 250 °C; Yield 78%, IR (KBr, cm^{-1}): 3421, 3345 (N–H stretching), 3063 (aromatic C–H stretching), 2966 (aliphatic C–H stretching), 1641 (C=N), 1578 (C=C), 1452 (CH_2 bending), 1216 (C–N). ^{1}H NMR (500 MHz, DMSO-d6) (δ, ppm): 0.67 (s, 9H, t-butyl), 1.98 (s, 1H, NH), 6.90 (t, J = 6.8 Hz, 1H, $H_{6''}$), 7.03 (t, J = 6.8 Hz, 1H, $H_{5''}$), 7.16 (t, J = 7.7 Hz, 1H, H_6), 7.22 (t, J = 7.7 Hz, 1H, H_7), 7.43 (d, J = 7.7 Hz, 1H, H_8), 7.48 (d, J = 8.2 Hz, 2H, $H_{3',5'}$), 7.52–7.55 (m, 3H, $H_{2',6',4''}$), 7.68 (d, J = 7.7 Hz, 1H, H_5), 8.35 (d, J = 6.8 Hz, 1H, $H_{7''}$), 11.61 (s, 1H, NH-indole). 13C NMR (125 MHZ, DMSO-d6) (δ, ppm): 29.3, 54.8, 111.2, 113.4, 115.2, 116.2, 118.1, 119.5, 120.3, 122.2, 122.9, 123.9, 124.1, 128.6, 128.8, 132.0, 132.2, 133.8, 136.3, 137.2, 141.2. MS (ESI) *m/z*: 415 (MH^+). Anal. Calcd for $C_{25}H_{23}ClN_4$ C, 72.37; H, 5.59; N, 13.50, Found C, 72.10; H, 5.37; N, 14.13.

N-tert-butyl-2-(2-(4-bromophenyl)-1H-indol-3-yl)H-imidazo[1,2-a]pyridin-3-amine (7p)

Cream powder, Mp > 250 °C; Yield 78%, IR (KBr, cm^{-1}): 3424, 3342 (N–H stretching), 3060 (aromatic C–H stretching), 2965 (aliphatic C–H stretching), 1626 (C=N), 1577 (C=C), 1452 (CH_2 bending), 1228 (C–N). ^{1}H NMR (500 MHz, DMSO-d6) (δ, ppm): 0.67 (s, 9H, t-butyl), 1.98 (s, 1H, NH), 6.86 (t, J = 6.8 Hz, 1H, $H_{6''}$), 7.03 (t, J = 6.8 Hz, 1H, $H_{5''}$), 7.14–7.19 (m, 2H, $H_{6,7}$), 7.43 (d, J = 7.9 Hz, 1H, H_8), 7.48–7.52 (m, 3H, $H_{3',5',4''}$), 7.62 (d, J = 7.9 Hz, 2H, $H_{2',6'}$), 7.68 (d, J = 7.9 Hz, 1H, H_5), 8.33 (d, J = 6.8 Hz, 1H, $H_{7''}$), 11.59 (s, 1H, NH-indole). 13C NMR (125 MHZ, DMSO-d6) (δ, ppm): 29.2, 54.8, 108.0, 110.9, 111.2, 116.5, 119.4, 120.4, 120.7, 122.1, 124.0, 128.6, 129.0, 129.1, 131.8, 132.6, 133.4, 133.7, 136.1, 136.4, 141.5. MS (ESI) *m/z*:

459 (MH+); Anal. Calcd for $C_{25}H_{23}BrN_4$ C, 65.36; H, 5.05; N, 12.20; Found C, 65.21; H, 5.25; N, 11.95.

4-(3-(3-(tert-butylamino)-5-methylH-imidazo[1,2-a]pyridin-2-yl)-1H-indol-2-yl) phenol (7q)

Creamish white powder, Mp > 250 °C; Yield 78%, IR (KBr, cm^{-1}): 3421 (O–H), 3337 (N–H stretching), 3060 (aromatic C–H stretching), 2967 (aliphatic C–H stretching), 1627 (C=N), 1578 (C=C), 1455 (CH_2 bending), 1226 (C–N), 1170 (C–O). ^{1}H NMR (500 MHz, DMSO-d6) (δ, ppm): 0.66 (s, 9H, t-butyl), 2.23 (s, 1H, NH), 2.78 (s, 3H, CH_3), 6.47 (d, J = 8.4 Hz, 1H, $H_{6''}$), 6.80 (t, J = 8.0 Hz, 1H, $H_{3',5'}$), 6.98–7.04 (m, 2H, $H_{6,7}$), 7.09 (t, J = 8.4 Hz, 1H, $H_{5''}$), 7.35 (d, J = 7.1 Hz, 1H, H_8), 7.38–7.41 (m, 3H, $H_{2',6',4''}$), 7.60 (d, J = 7.1 Hz, 1H, H_5), 9.63 (s, 1H, OH), 11.63 (s, 1H, NH-indole). ^{13}C NMR (125 MHZ, DMSO-d6) (δ, ppm): 21.53, 29.45, 53.59, 110.6, 112.4, 115.7, 120.7, 121.7, 122.9, 124.9, 125.6, 127.3, 128.8, 130.4, 131.2, 132.8, 134.1, 135.7, 137.9, 138.1, 142.7, 152.8. MS (ESI) *m/z*: 411 (MH+); Anal. Calcd for $C_{26}H_{26}N_4O$ C, 76.07; H, 6.38; N, 13.65; Found C, 76.29; H, 6.13; N, 13.47.

N-tert-butyl-2-(2-(4-chlorophenyl)-1H-indol-3-yl)-5-methylH-imidazo[1,2-a] pyridin-3-amine (7r)

Creamish white powder, Mp: 245–247 °C; Yield 71%, IR (KBr, cm^{-1}): 3343 (N–H stretching), 3061 (aromatic C–H stretching), 2968 (aliphatic C–H stretching), 1628 (C=N), 1582 (C=C), 1453 (CH2 bending), 1233 (C–N). ^{1}H NMR (500 MHz, DMSO-d6) (δ, ppm): 0.58 (s, 9H, t-butyl), 1.98 (s, 1H, NH), 2.86 (s, 3H, CH_3), 6.57 (d, J = 7.2 Hz, 1H, $H_{6''}$), 7.03–7.09 (m, 2H, $H_{6,7}$), 7.16 (t, J = 7.2 Hz, 1H, $H_{5''}$), 7.37 (d, J = 8.8 Hz, 1H, H_8), 7.43 (d, J = 7.2 Hz, 1H, $H_{4''}$), 7.56 (d, J = 8.0 Hz, 2H, $H_{3',5'}$), 7.62–7.65 (m, 3H, $H_{2',6',5}$), 11.58 (s, 1H, NH-indole). 13C NMR (125 MHZ, DMSO-d6) (δ, ppm): 20.0, 28.9, 54.2, 108.7, 111.3, 113.3, 114.7, 115.0, 119.6, 120.2, 120.7, 122.2, 123.5, 128.9, 131.8, 132.3, 133.4, 133.6, 136.1, 136.2, 136.5, 142.8; MS (ESI) *m/z*: 429 (MH^+). Anal. Calcd for $C_{26}H_{25}N_4$ C, 72.80; H, 5.87; N, 13.06; Found C, 73.05; H, 6.0; N, 12.89.

N-tert-butyl-2-(2-(4-bromophenyl)-1H-indol-3-yl)-5-methylH-imidazo[1,2-a] pyridin-3-amine (7s)

Creamish white powder, Mp > 250 °C; Yield 71%, IR (KBr, cm^{-1}): 3341 (N–H stretching), 3059 (aromatic C–H stretching), 2965 (aliphatic C–H stretching), 1625 (C=N), 1580 (C=C), 1456 (CH_2 bending), 1234 (C–N). ^{1}H NMR (500 MHz, DMSO-d6) (δ, ppm): 0.58 (s, 9H, t-butyl), 1.98 (s, 1H, NH), 2.86 (s, 3H, CH_3), 6.57 (d, J = 7.4 Hz, 1H, $H_{6''}$), 7.03–7.09 (m, 2H, $H_{6,7}$), 7.16 (t, J = 7.4 Hz, 1H, $H_{5''}$), 7.36 (d, J = 8.8 Hz, 1H, H_8), 7.43 (d, J = 7.4 Hz, 1H, $H_{4''}$), 7.56 (d, J = 8.1 Hz, 2H, $H_{3',5'}$), 7.61–7.64 (m, 2H, $H_{2',6',5}$), 11.57 (s, 1H, NH-indole). 13C NMR (125 MHZ, DMSO-d6) (δ, ppm): 20.3, 28.9, 54.3, 108.6, 113.2, 115.0, 115.1, 119.6, 120.3, 120.7, 121.1, 122.2, 122.3, 123.6, 126.1,

129.0, 131.7, 131.8, 132.2, 136.1, 136.6, 142.8. MS (ESI) *m/z*: 473 (MH^+); Anal. Calcd for $C_{26}H_{25}BrN_4$ C, 65.96; H, 5.32; N, 11.83; Found C, 65.79; H, 5.20; N, 12.15.

N-tert-butyl-5-methyl-2-(2-p-tolyl-1H-indol-3-yl)H-imidazo[1,2-a]pyridin-3-amine (7t)

Creamish white powder, Mp > 250 °C; Yield 77%, IR (KBr, cm^{-1}): 3338 (N–H stretching), 3026 (aromatic C–H stretching), 2965 (aliphatic C–H stretching), 1625 (C=N), 1577 (C=C), 1453 (CH_2 bending), 1217 (C–N). ^{1}H NMR (500 MHz, DMSO-d6) ($\boldsymbol{\delta}$, ppm): 0.58 (s, 9H, t-butyl), 2.19 (s, 1H, NH), 2.32 (s, 3H, CH_3), 2.82 (s, 3H, CH_3), 6.56 (d, J = 7.1 Hz, 1H, $H_{6''}$), 7.02–7.09 (m, 2H, $H_{6,7}$), 7.14 (t, J = 7.1 Hz, 1H, $H_{5''}$), 7.24 (d, J = 7.3 Hz, 2H, $H_{3',5'}$), 7.37 (d, J = 8.2 Hz, 1H, H_8), 7.41 (d, J = 7.1 Hz, 1H, $H_{4''}$), 7.47 (d, J = 7.3 Hz, 2H, $H_{2',6'}$), 7.70 (d, J = 8.2 Hz, 1H, H_5), 11.45 (s, 1H, NH-indole). 13C NMR (125 MHZ, DMSO-d6) (δ, ppm): 20.2, 20.7, 28.7, 54.4, 107.5, 111.0, 113.1, 115.0, 119.4, 120.1, 121.7, 123.3, 125.8, 126.8, 126.9, 128.9, 129.5, 130.4, 135.0, 136.4, 136.7, 137.1, 142.8. MS (ESI) *m/z*: 409 (MH^+); Anal. Calcd for $C_{27}H_{28}N_4$ C, 79.38; H, 6.91; N, 13.71; Found C, 79.21; H, 7.05; N, 13.64.

Biology

Anti-proliferative assay

The cytotoxic activity of the synthesized compounds **7a**–**7t** was assessed against three different cancer cell lines [31]. Tumor cell lines including lung cancer cell line (*A-549*), liver cancer cell line (*Hep-G2*), breast cancer cell line (*MCF-7*) and epithelial substrain cell line (*TD-47*) were obtained from the National Cell Bank of Iran and grown in RPMI-1640 medium (Gibco, UK). Exponentially growing cells (1×10^4 cells/well) were seeded in 96-well with in RPMI1640 medium at 37 °C under 5% CO_2 supplemented with 10% FBS, 1% L-glutamine, and penicillin–streptomycin, and incubated overnight. The cells were treated by different concentrations of test compounds and allowed to incubate for 48 h in a humidified atmosphere. All compounds were initially dissolved in DMSO, and the final concentration of DMSO was less than 1% in all the concentrations of the applied compounds. Etoposide and colchicine were used as positive controls. After 48 h of further incubation, the medium was replaced with MTT (1 mg/mL), followed by 4 h incubation. After the formation of blue formazan crystals, the culture medium was replaced with 100 µL of DMSO and the absorbance values were measured using a multi-well plate reader (Gen5; Epoch, BioTek, USA) at 492-nm wavelength. The IC_{50} values were compared with the control and expressed in mean ± SD from the dose–response logarithmic curves of at least three independent experiments.

Acridine orange/ethidium bromide double staining

Apoptosis in the treated cancer cells was determined morphologically after staining with acridine orange/ethidium bromide using fluorescence microscopy (Zeiss,

Germany) [31]. *A-549* cells grown in 12-well plates (5×10^5 cells/well) were treated with and without IC_{50} concentrations of compound **7a** and **7f** for 24 h. Then, the cells were washed three times with PBS. Finally, ethidium bromide/acridine orange (1:1, 100 mg/mL) solution was added to the cell suspension, and the nuclear morphology was evaluated by fluorescence microscopy. All the experiments were repeated three times.

Flow cytometry analysis of the apoptotic cells with Annexin V-FITC/PI staining

Flow cytometry analyses for **7a** and **7f** were performed to confirm apoptosis induced in comparison with the standard drug etoposide [31]. In brief, 5×10^5 cells/well of *A-549* were treated with the IC_{50} doses of the most potent compounds, **7a** and **7f**. After 24 h, the cells were washed twice with cold PBS, collected by centrifugation and resuspended in 1× annexin V binding buffer [0.1 M Hepes/NaOH (pH 7.4), 1.4 M NaCl, 25 mM $CaCl_2$]. Then, the cells were double-stained with 5 µL of annexin V-FITC and 5 µL of PI, and the cells were gently vortexed and incubated at room temperature for 15 min in the dark before flow cytometry. Finally, 400 µL of 1× annexin binding buffer was added into the suspension, and the cells were analyzed using a flow cytometer within 1 h.

Molecular docking study

Computer-simulated docking studies were accomplished by the AutoDock 4.2 software. The Lamarckian Genetic Algorithm of the AutoDock 4.2 program was used as the search algorithm. The Graphical User Interface program, AutoDock Tools 1.5.6 was used to prepare, run, and analyze the docking simulations. Molecular docking of compounds was performed with two crystal structures (PDB ID: 1SA0 and 1ZXM for tubulin and topoisomerase II, respectively) by the Auto-Dock Tools 1.5.6. All two-dimensional structures of the compounds were built using ChemDraw Ultra 10.0 (Cambridge Software), and then moved into the Hyperchem 8.0 software (Release 8.0 for Windows, Molecular Modeling System, HyperCube 2007). Molecules were subjected to energy minimization with MM + force field and then the PM3 semi-empirical technique. Then, the partial charges of the atoms were calculated by the Gasteiger–Marsili procedure implemented in the AutoDock Tools package [32]. The non-polar hydrogens of compounds were merged and then the crystal structures of protein were taken from the Protein Data bank (www.rcsb.org). All bound water and ligands were eliminated from the protein, and polar hydrogen atom were added to the protein as it was required for the electrostatics interactions, and then non-polar hydrogen atoms were merged. In all the dockings, a grid map with 60 grid points in the *X*, *Y*, and *Z* directions was built. Among the three different search algorithms offered by AutoDock 4.2, the Lamarckian genetic algorithm approach was applied. For all docking procedures, 100 independent runs with step sizes of 0.2 Å for translations and 5° for orientations and torsions were considered. For the Lamarckian genetic algorithm method, a maximum number of 25×10^5 energy evaluations, 27,000 maximum generations, a gene mutation rate of 0.02. and

a cross-over rate of 0.8 were used. At the end of docking, the structures were ranked by energy. Ligand–receptor interactions were all visualized on the basis of the docking results using Discovery Studio Visualizer 4.0.

Results and discussion

Chemistry

The overall procedure for the synthesis of the designed compounds **7a–t** is illustrated in Scheme 1 (above). As illustrated in this scheme, the reaction of acetophenone derivatives and phenyl hydrazine in the presence of acetic acid and polyphosphoric acid in refluxing EtOH afforded 2-aryl-1H-indoles **3a–f** in good yield. Subsequently, treatment of compounds **3a–f** with phosphorous oxychloride in DMF led to 2-aryl-1H-indole-3-carbaldehyde derivatives **4a–f** [27]. Finally, compound **4**, 2-aminopyridines and isocyanides were refluxed in toluene to generate imidazopyridines-linked 2-aryl-1H-indoles **7a–t** in a good yield.

The structures of the title compounds **7a–t** were determined by ^{1}H and ^{13}CNMR, IR and elemental analyses. As exemplified with the IR analysis of N-cyclohexyl-2-(2-p-tolyl-1H-indol-3-yl)H-imidazo[1,2-a]pyridin-3-amine (**7f**) displayed major adsorption bands at 1624 cm^{-1} and 1225 cm^{-1}, which were due to the stretching vibrations of C=N and C–N bonds, respectively. Furthermore, two bands were observed at 3351 and 3131 cm^{-1} which were assigned to the ν(N–H) stretching of compound **7f**.

The ^{1}H NMR spectrum for compound **7f** showed protons resonance at 6.85–8.18 ppm, which was due to the aromatic, pyridine and indole rings. In addition, two single resonances for the NH groups appeared at 1.99 and 11.47 ppm, which were due to the cyclohexyl and indole rings, respectively. Also, the signals related to the protons of the cyclohexyl group appeared at 0.9–0.91 ppm, 1.26–1.31 ppm, and a multiplet at 3.07–3.08 ppm for CH–N of the cyclohexyl ring. Finally, the single resonance at 2.3 ppm was related to the methyl group as R_1.

Biological

Anti-proliferative activity

Derivatives of series **7a–t** were synthesized and screened against A-549 (lung), Hep-G2 (liver), MCF-7 and T-47D (breast) cell lines (Table 1). As shown in Table 1, compound **7f**, having the N1-cyclohexyl-imidazo[1,2-a]pyridin-3-amine moiety substituted on the C-3 position of the indole ring and the tolyl ring at the C-2 position, exhibited the highest inhibitory activity against A-549 with $IC_{50} = 10.34$ μM, which was more potent than etoposide ($IC_{50} = 36.72$ μM) and other synthesized derivatives. Compound **7d** with the N1-cyclohexyl-imidazo[1,2-a]pyridin-3-amine moiety substituted on the C-3 position of the indole ring and the *para* chloro phenyl ring at the C-2 position, exhibited the

Table 1 Cytotoxic activities of the synthesized compounds against MCF-7, A549, HepG2 and T-47D cell lines

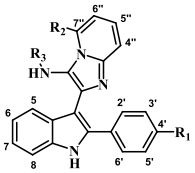

Compound	R_1	R_2	R_3	[a]A-549	[a]Hep-G2	[a]T-47D	[a]MCF-7
7a	H	H	Cyclohexyl	11.48 ± 3.29	66.34 ± 5.40	> 100	> 100
7b	OH	H	Cyclohexyl	> 100	> 100	> 100	> 100
7c	OMe	H	Cyclohexyl	36.57 ± 2.81	44.27 ± 4.89	> 100	> 100
7d	Cl	H	Cyclohexyl	25.67 ± 3.03	35.79 ± 2.03	> 100	> 100
7e	Br	H	Cyclohexyl	16.44 ± 4.41	43.94 ± 6.70	> 100	> 100
7f	Me	H	Cyclohexyl	10.66 ± 2.85	51.59 ± 2.92	> 100	> 100
7g	OH	Me	Cyclohexyl	21.26 ± 3.89	41.55 ± 7.42	92.92 ± 7.51	69.40 ± 4.39
7h	OMe	Me	Cyclohexyl	34.36 ± 2.97	47.97 ± 6.43	83.42 ± 8.70	65.22 ± 3.68
7i	Cl	Me	Cyclohexyl	> 100	49.85 ± 3.18	> 100	> 100
7j	Br	Me	Cyclohexyl	94.91 ± 8.70	37.37 ± 0.70	69.35 ± 13.07	49.69 ± 2.49
7k	Me	Me	Cyclohexyl	46.56 ± 4.95	45.56 ± 2.41	> 100	77.98 ± 6.44
7l	H	H	t-butyl	> 100	> 100	> 100	> 100
7m	OH	H	t-butyl	> 100	> 100	> 100	> 100
7n	OMe	H	t-butyl	35.27 ± 5.26	44.17 ± 5.23	> 100	> 100
7o	Cl	H	t-butyl	63.50 ± 7.78	60.20 ± 2.29	> 100	82.98 ± 5.31
7p	Br	H	t-butyl	32.84 ± 4.63	48.36 ± 4.85	> 100	> 100
7q	OH	Me	t-butyl	> 100	> 100	> 100	> 100
7r	Cl	Me	t-butyl	51.89 ± 1.23	> 100	> 100	> 100
7s	Br	Me	t-butyl	> 100	> 100	> 100	> 100
7t	Me	Me	t-butyl	> 100	> 100	> 100	> 100
Colchicine	–	–	–	1.76 ± 0.19	5.93 ± 0.48	7.1 ± 1.10	4.96 ± 0.97
Etoposide	–	–	–	39.18 ± 1.96	37.13 ± 1.73	33.89 ± 1.45	37.76 ± 2.18

[a]The IC50 (half-maximal inhibitory concentration) values (μM) represent an average of three independent experiments (mean ± SD)

highest inhibitory activity against Hep-G2 with $IC_{50} = 35.79$ μM compared with etoposide ($IC_{50} = 37.13$ μM) and colchicine ($IC_{50} = 1.76$ μM). However, compound **7j**, having the N1-cyclohexyl-5-methyl-imidazo[1,2-a]pyridin-3-amine at the C-3 position of the indole ring and the *para* bromo phenyl ring at the C-2 position, had the highest inhibitory activity against T-47D and MCF-7 cell lines with $IC_{50} = 69.35$ μM and 49.69 μM, respectively. All compounds showed higher activity against the two A-549 and Hep-G2 cell lines than against other cell lines.

MCF-7 (breast cancer) cell line: Compound **7j** was found to be the most potent one against the MCF-7 cell line among the studied compounds. Others had weak cytotoxic activity against this cell line. Replacement of the cyclohexyl ring as R_3 in the structure of **7g–k** with the t-butyl group giving **7q–t** led to a decrease of cytotoxic activity against the MCF-7 cell line (Table 1). The presence of the cyclohexyl group substituted on the amine group of the imidazopyridyl moiety and the more lipophilic halogen group at the *para* position of the phenyl ring in the structure of compound **7j** have important roles in inhibitory activity against the MCF-7 cell line. However, all compounds showed weaker activity than colchicine and etoposide drugs against the MCF-7 cell line.

A-549 (lung cancer) cell line: Compounds **7a** and **7f** exhibited the highest cytotoxic activity ($IC_{50} = 11.48$ μM and 10.66 μM, respectively) against the A-549 cell line. Here again, compounds having the cyclohexyl group substituted on the amine group of the imidazopyridyl moiety showed higher activity against the A-549 cell line than compounds bearing the t-butyl amine group at the same position (Table 1). Among the studied compounds, those with the cyclohexyl ring and hydrogen substitution as R_3 and R_2, respectively, the cytotoxic activity order was **7f > 7a > 7e > 7d > 7c > 7b**. This order can be explained by the lipophilicity of the groups substituted on the phenyl ring at C-2 of the indole ring. Moreover, between the compounds with the t-butyl group substituted on the imidazopyridyl moiety, a compound with the *para* bromo phenyl ring at C-2 of the indole ring, **7p** showed the highest activity among the other compounds. According to the results in this series, the presence of lipophilic groups at the phenyl ring at the C-2 indole ring moiety had a positive effect. Compounds **7a–h** (except for **b**) showed more potent cytotoxic activity compared with etoposide ($IC_{50} = 10.66$–36.57 μM vs. 39.18 μM). Furthermore, replacing hydrogen with methyl at the imidazopyridyl moiety decreased activity against the A-549 cell line.

Hep-G2 (liver cancer) cell line: Here again, compounds having the cyclohexyl amine substituted on the imidazopyridyl moiety showed higher activity than compounds bearing the t-butyl amine group at the same position (Table 1). Compound **7d** ($R_1 = Br$ and $R_3 =$ cyclohexyl) revealed the highest inhibitory activity against the Hep-G2 cell line ($IC_{50} = 36.12$ μM). The presence of a lipophilic group substituted on the phenyl ring at the C-2 position of the indole ring resulted in higher activity against the Hep-G2 cell line. Replacement of the chloro group (**7d**) in the *para* position of the phenyl ring with methoxy (**7c**) or hydroxyl (**7b**) led to a decrease in the cytotoxicity. Compounds **7q–t** demonstrated no cytotoxic activity against this cell line ($IC_{50} > 100$). Interestingly, the presence of methyl at the R_2 and *tert*-butyl at the R_3 positions drastically decreased cytotoxicity against the Hep-G2 cell line.

T-47D (breast cancer) cell lines: None of the synthesized compounds demonstrated cytotoxicity against the T-47D cell line ($IC_{50} > 100$), except **7g**, **7h** and **7j** which showed $IC_{50} = 92.92$, 83.42 and 69.35 μM, respectively. Among these compounds, **7j** revealed the most potent activity in this series against the T-47D cell

line (Table 1). Based on structure–activity relationships of these compounds, the presence of a lipophilic group (e.g., Br) on the phenyl ring at the C-2 position of the indole ring had a toxic effect against the T-47D cell line. Compounds with the cyclohexyl ring as R_3 and the methyl group as R_2 showed higher toxicity against this cell line compared with the other compounds. On the whole, all the prepared compounds were less cytotoxic against T-47D compared with other cell lines.

To further assess the cytotoxic effects of the synthesized compounds, compounds **7a** and **7f** (the most potent compounds against A-549), were evaluated against the normal human cell lines HDF. The results revealed that these compounds were non-cytotoxic at 100-μM concentrations to the studied normal cells.

Morphological analysis

The morphological assessment of the A-549 cells by the acridine orange/ethidium bromide double-staining method was used to reveal the potential of compounds **7a** and **7f** as apoptotic inducers [28]. Living cells have a normal green nucleus, but apoptotic cells show orange-stained nuclei with chromatin condensation or fragmentation. Accordingly, compounds **7a** and **7f** were investigated in comparison with etoposide for identification of apoptosis induced in A-549 cells.

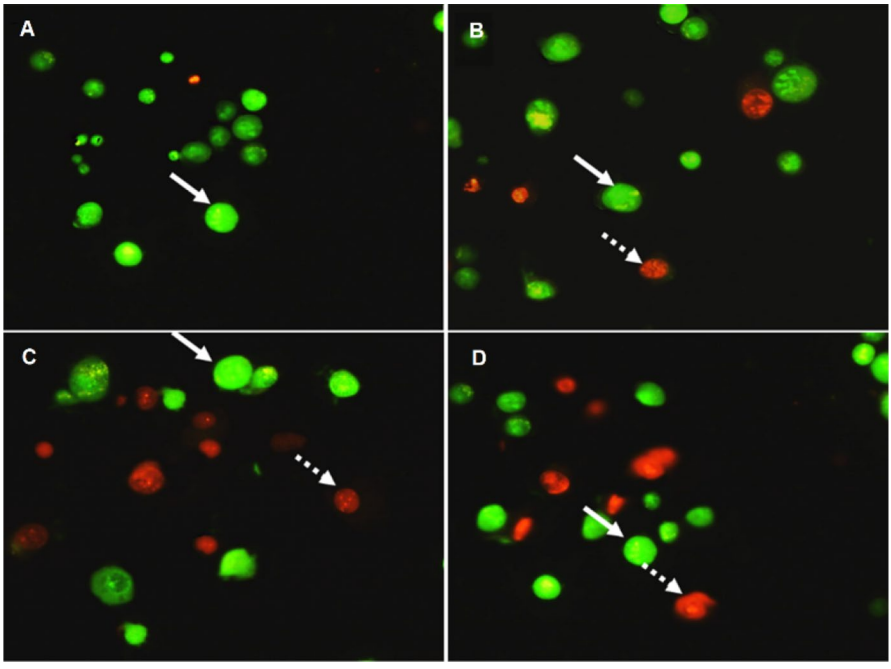

Fig. 2 Acridine orange/ethidium bromide double-staining of cancer cells with characteristic symptoms of apoptosis of A-549. **a** DMSO 1% as control, **b**–**d** cells treated with IC_{50} concentrations of etoposide, compounds **7a** and **7f**, respectively, for 24 h. *White arrows* indicate live cells, *dashed arrows* show apoptosis. The images of the cells were taken with a fluorescence microscope at magniciation of ×400

Analysis of the acridine orange/ethidium bromide double-staining of the selected most potent compounds, **7a** and **7f**, in the A-549 cell line is shown in Fig. 2, in which the viable cells are observed to be green but the apoptotic cells with chromatin condensation or fragmentation show orange-stained nuclei. Morphological findings indicated that compounds **7a** and **7f** reduced cell viability and induced apoptosis in A-549 cells. The lung cancer cells treated with **7a** and **7f** showed higher apoptosis compared with etoposide as the reference drug.

Flow cytometry analysis

The apoptosis induction caused by the prepared compounds was also confirmed by flow cytometry analysis. Annexin V-FITC/PI was used as a quantitative method for determining apoptosis. The results indicated that the prepared compounds could induce apoptosis in A-549 cancer cells. Flow cytometric analysis revealed that cells

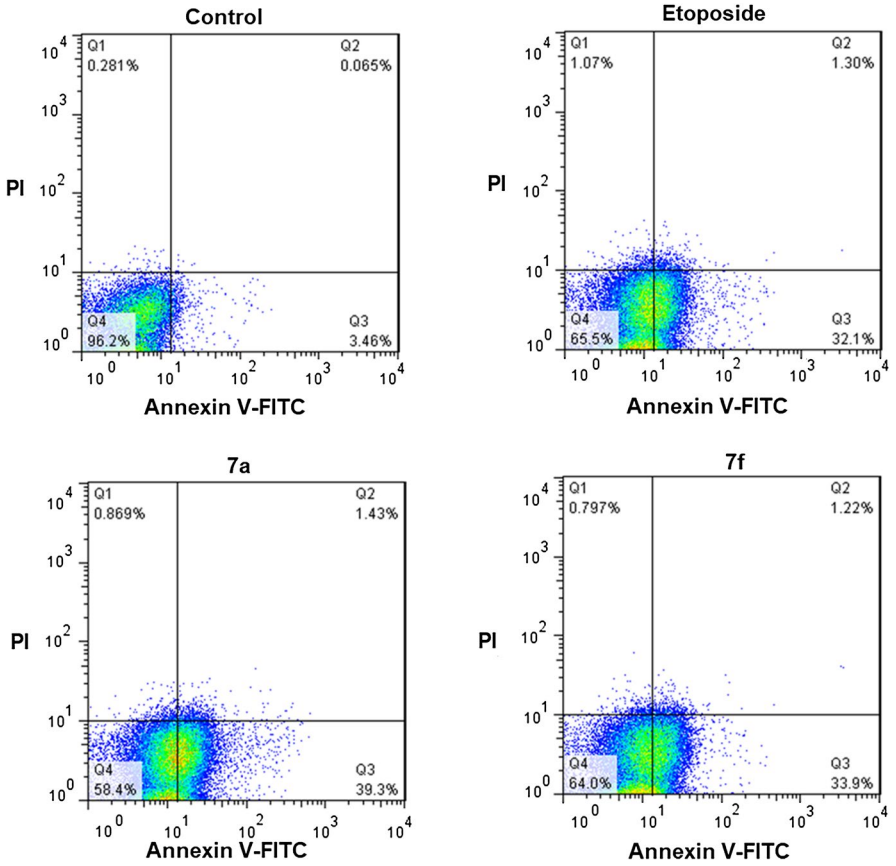

Fig. 3 Flow cytometric analysis of A-549 cells treated with the prepared compounds **7a** and **7f**. Cells were stained with annexin V-FITC/PI and quantitated by flow cytometry. Cells were treated with DMSO 1% (negative control) or with IC_{50} values of etoposide (positive control)

undergo apoptosis after treatment with the test compounds. As illustrated in Fig. 3, the apoptotic index of compound **7a** and **7f** was compared with the negative control and etoposide in the A-549 cells. Double-staining followed by flow cytometric analysis revealed the percentages of apoptotic cells as 39.3% and 33.9% resulting from the treatment with compounds **7a** and **7f** after 24 h incubation, respectively. In addition, the corresponding value obtained after the treatment with etoposide was 32.1% following 24 h incubation (Fig. 3).

Molecular docking study

Molecular docking as an important method in structure-based computer-assisted drug design for predicting the main binding mode(s) of a ligand with a protein of known three-dimensional structure [29]. Molecular docking simulations and analysis of the binding modes of the designed compounds within tubulin and ATPase domain of topoisomerase IIα active sites were performed to rationalize the anticancer activity results. At first, the binding sites of colchicine and adenylyl-imidodiphosphate (ANP) were precisely characterized inside the active site of tubulin and the ATPase domain of topoisomerase IIα, respectively (Fig. 4). The formation of hydrogen bonds between the carbonyl group attached to the cycloheptyl ring of colchicine and NH of Val181, as well as the methoxy group and the SH group of Cys241, can be seen in Fig. 4a,. In addition, hydrophobic interactions of different parts of colchicine with Lys352, Val315, Ala180, Met259, Leu255, Leu248, Ala250, and Asn258 have been well established. Figure 4b also clearly represents the hydrogen bonding interaction of some parts of ANP with Gly166, Tyr165, Asn163, Ser149, Gln376, Asn150, Asn91, Arg162, and Asn120 residues. Hydrophobic interactions of ANP with Lys168, Ala167, Lys378, Gly161, Arg1 and Asp94 have also been fully recognized, as indicated in Fig. 4.

Docking studies revealed that the binding modes of the most active compounds are coherent with colchicine and ANP.

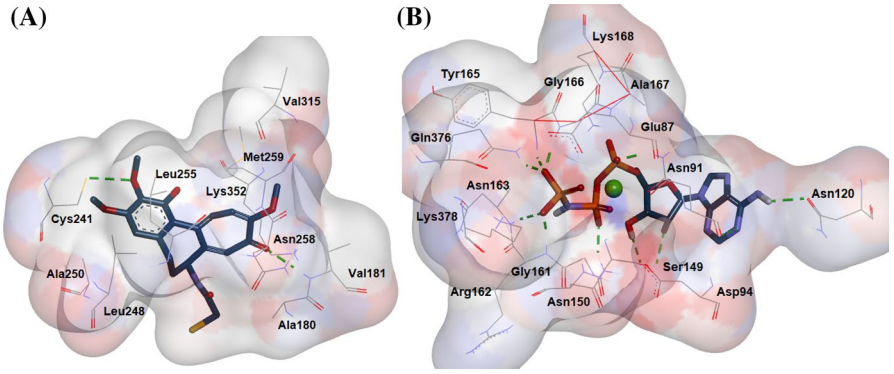

Fig. 4 Binding sites of **a** colchicine and **b** ANP in the active site of tubulin and ATPase domain of topoIIα. *Green dashed lines* indicate hydrogen bonds

Binding mode of the prepared compounds

Molecular interactions established for the studied compounds inside the ATPase domain of topoisomerase IIα and tubulin obtained by molecular docking protocol are summarized in Tables 2 and 3, respectively.

Compounds **7c** with methoxy at the *para* phenyl ring and cyclohexyl as R_3, and **7j** bearing bromo at the *para* phenyl ring again with cyclohexyl as R_3 showed the highest free binding energy at topoisomerase IIα and tubulin active sites, respectively (Tables 2, 3). It seemed that the *para* methoxy- and *para* bromo-substituted phenyl might be responsible for additional hydrophobic interactions with the topoisomerase IIα and tubulin. In antiproliferative activity assay, compound **7c** showed weak activity against T-47D and MCF-7 cell lines (Table 1), whereas **7j** showed the highest activity against the Hep-G2, T-47D and MCF-7 cell lines among the compounds with $R_2 = CH_3$ and $R_3 =$ cyclohexyl. Moreover, this compound showed moderate activity against Athe -549 cell line in biological assays, as shown in Table 1.

Compound **7c** was involved in hydrophobic interactions with the side chains of Ala92, Asn91, Thr159, Asp94, Ser149, Ile125, Gly164, Gly166, Ala167 and Thr147 residues of topoisomerase IIα. In addition, the carbonyl group of Asn95 formed a hydrogen bond with the hydrogen of NH attached to the imidazopyridine moiety. The amine group of Lys168 formed a hydrogen bond with the methoxy group of the phenyl moiety in **7c**. This can be seen in Fig. 5 for compounds **7c** and **7j** inside both the active sites. Moreover, compound **7j** interacts hydrophobically with Asn150, Asn91, Asn95, Thr215, Thr147, Asp94, Ser148, Arg98, Ser149 and Ile141 residues in topoisomerase IIα. However, this compound did not show any hydrogen bond with the active site residues, as can be seen in Fig. 5. Neither of the compounds **7c** and **7j** displayed any hydrogen bond in the tubulin protein. However, these two compounds interact with Leu255, Ala250, Asn249, Lys254, Leu248, Asn258, Met259, Ala316, Lys352, Thr353 and Ala317 residues inside the tubulin active site in a hydrophobic manner (Fig. 5).

Compound **7f** revealed the highest activity among the first series against the A-549 cell line according to the antiproliferative activity assay (10.66 μM). Compound **7f** did not show any hydrogen bonding with the amino acids at the tubulin active site, whereas the NH group of this compound exhibited a hydrogen bond with the carbonyl group of the Asn95 residue. Docking studies showed that the steric orientation of **7f** was similar to colchicine and ANP inside their corresponding active sites. This can be seen in Fig. 6 by superimposing **7f** with ANP and colchicine inside both the active sites.

Replacing the cyclohexyl ring of **7a–k** with the t-butyl group of **7l–t** (R_3) revealed a decrease in the free binding energy at both active sites. For example, compound **7c** with the cyclohexyl ring showed the highest free binding energy, while compound **7n** bearing the t-butyl group showed the lowest free binding energy, as can be seen in Table 2. This can be explained by the higher hydrophobicity of compound **7c** compared to **7n** due to the greater lipophilicity of the cyclohexyl ring. The docking results also revealed that all the compounds except **7g** and **7q** formed cation–π stacking interactions with Lys168, Arg98 and Lys157

Table 2 Estimated free binding energy, hydrogen bonds, hydrophobic, and cation–π interactions obtained for the best-docked conformations of the studied compounds inside the ATPase domain of topoisomerase IIα inhibitors

Compound	$\Delta G_{binding}$	Hydrogen bond interaction	Hydrophobic interaction	Cation–π interaction
7a	−9.95	Asn120, Asn91	Asn150, Thr159, Asp94, Lys123, Arg98, Ile125, Thr215, Asn95, Phe142, Ala167, Gly124, Ile88, Ile118, Ile217, Ala92	Arg98
7b	−9.53	Asn91, Lys168, Thr147	Ile217, Thr215, Phe142, Asn120, Ala167, Asp94, Asn95, Gly164, Ile125, Ile141, Arg98, Ser149, Pro126	Lys168
7c	−10.09	Lys168, Asn95	Ala92, Asn91, Thr159, Asp94, Ser149, Ile125, Gly164, Gly166, Ala167, Thr147	Lys168, Arg98
7d	−9.73	Asn95	Thr147, Ala167, Ile141, Phe142, Asn91, Thr215, Ala92, Ile125, Pro126, Arg98, Asp94, Asn120, Thr159, Asn150, Ser149	Lys168
7e	−9.98	Asn95	Ser148, Thr147, Asn91, Thr215, Asn120, Ile141, Pro126, Ile125, Arg98, Asn150, Ala92, Thr159, Asp94, Ser149	Lys168
7f	−9.41	Asn95	Lys168, Ala167, Thr147, Ile141, Asn150, Phe142, Ser149, Asn91, Ala92, Pro126, Thr215, Asn120, Ile125, Thr159, Arg98, Asp94	Arg98
7g	−9.61	Ile141, Asn95, Ser149	Ser148, Asn120, Asn150, Asn91, Asp94, Thr215, Ile125, Thr159, Arg98, Thr147, Lys168	–
7h	−9.51	Ser149	Lys168, Phe142, Thr147, Ile141, Ser148, Pro126, Ile125, Ala167, Asn120, Asp94, Thr215, Asn95, Asn91, Arg98, Ala92	Arg98, Lys168
7i	−9.66	Ser149	Asp94, Thr215, Arg98, Asn95, Asn91, Pro126, Thr159, Asn150, Gly164, Thr147, Lys157, Ile141, Ser148, Ile125	Lys157
7j	−9.85	–	Asn150, Asn91, Asn95, Thr215, Thr147, Asp94, Gly164, Arg98, Ile125, Ile141, Ser149	Lys157
7k	−9.57	Ser149	Thr215, Asn95, Asn120, Asn91, Asp94, Gly164, Thr147, Thr159, Lys157, Arg98, Ile125, Asn150, Pro126, Ile141, Ser148	Asn91, Lys157
7l	−8.72	Asn91	Asn95, Asp94, Ser149, Phe142, Ala167, Ile88, Thr215, Ile125, Arg98, Gly125, Lys123, Ala92, Ile217, Ile118	Arg98
7m	−8.64	Lys168	Ser149, Arg98, Ile125, Asn120, Asp94, Pro126, Ala92, Asn91, Ile141, Phe142, Ala167	Arg98
7n	−8.50	Lys168	Ile125, Ser149, Arg98, Asp94, Asn95, Ala92, Asn120, Thr215, Ile141, Asn91, Phe142, Tyr165, Gly164, Ala167, Gly166, Thr147	Lys168, Arg98

Table 2 (continued)

Compound	$\Delta G_{binding}$	Hydrogen bond interaction	Hydrophobic interaction	Cation–π interaction
7o	−8.89	–	Ser149, Asn95, Asp94, Pro126, Ile125, Asn120, Ile141, Thr215, Arg98, Asn91, Ala92, Thr147, Ala167	Arg98
7p	−9.01	–	Ser148, Thr147, Lys123, Ile125, Arg98, Asn95, Thr215, Phe142, Asp94, Lys168, Ile141, Asn91, Ala167, Ile217	Lys168
7q	−8.78	Lys168, Ile141	Asp94, Asn120, Asn95, Ile125, Arg98, Lys123, Thr215, Thr159, Asn91, Asn150, Ser149, Ala167	–
7r	−8.70	–	Lys123, Gly124, Ile125, Pro126, Thr215, Ile141, Asn120, Asn95, Ser148, Lys157, Asp94, Asn150, Arg98, Thr159, Gln97	Lys157
7s	−8.87	Ser149	Asn150, Thr159, Lys157, Ile141, Gly161, Ser148, Gly164, Asn95, Arg98, Asp94, Thr215, Asn91, Thr147	Lys157
7t	−8.67	–	Thr147, Ile141, Pro126, Ile125, Gly124, Thr215, Asn91, Asn95, Lys123, Asn120, Ser148, Arg98, Thr159, Asn150, Gln97, Asp94	Lys157
ANP	−13.96	Asn91, Asn163, Arg162, Gln376, Gly166, Ser149, Asn150, Asn120, Tyr165,	Gly161, Lys378, Asp94, Lys168, Ala167, Arg162	–

Table 3 Estimated free binding energy, hydrogen bonds, hydrophobic, and cation–π interactions obtained for the best-docked conformations of the studied compounds inside tubulin

Compound	$\Delta G_{binding}$	Hydrogen bond interaction	Hydrophobic interaction	Cation–π interaction
7a	−10.46	–	Lys352, Ala354, Thr353, Ala317, Lys254, Ala250, Val238, Cys241, Leu248, Leu255, Leu242, Asn258, Met259, Ala316	–
7b	−9.84	Thr179, Lys352	Lys254, Val315, Thr314, Cys241, Leu255, Asn258, Met259, Ala316, Val181, Lys352, Val318, Ala354, Asn350, Leu248, Ser178	–
7c	−10.39	–	Ala317, Ala250, Leu252, Leu255, Thr353, Leu248, Asn249, Lys254, Ala316, Lys352, Val315, Met259, Asn258, Ala316, Ala317	–
7d	−10.59	–	Lys254, Asn249, Ala250, Leu242, Leu248, Cys241, Leu255, Asn258, Met259, Ala354, Thr353, Ala317, Ala316, Lys352	–
7e	−10.80	–	Asn258, Val181, Met259, Asn249, Ala250, Leu242, Leu248, Lys254, Leu255, Cys241, Ala354, Lys352, Ala316, Thr353, Ala317	–
7f	−10.46	–	Ala250, Cys241, Leu248, Leu255, Leu242, Met259, Asn258, Asn249, Lys254, Val238, Ala316, Lys352, Thr353, Ala317, Ala354	–
7g	−10.03	Asn258	Cys241, Ala250, Thr353, Ala317, Ala316, Ala354, Lys352, Leu248, Val238, Leu255, Leu242, Met259, Lys254, Asn249	–
7h	−10.57	–	Val315, Asn258, Met259, Cys241, Asn249, Lys254, Ala316, Leu242, Leu255, Val238, Thr353, Leu248, Ala250, Ala354, Lys352, Ala317	–
7i	−10.70	–	Ala250, Asn258, Met259, Leu242, Val238, Leu255, Leu248, Lys254, Asn249, Cys241, Ala354, Ala317, Lys352, Thr353, Ala316	–
7j	−10.94	–	Ala317, Ala250, Leu252, Leu255, Thr353, Leu248, Asn249, Lys254, Ala316, Lys352, Val315, Met259, Asn258, Ala316, Ala317	–
7k	−10.64	–	Met259, Asn258, Lys254, Asn249, Ala250, Leu248, Val238, Leu242, Leu255, Ala354, Lys352, Thr353, Cys241, Ala316, Ala317	–
7l	−9.35	–	Cys241, Ala250, Ala354, Lys352, Ala316, Ala317, Thr353, Met259, Asn258, Lys254, Leu255, Leu242, Val238, Leu248	–
7m	−9.33	Val315, Asn350	Cys241, Ala354, Leu255, Ala316, Val318, Lys352, Lys254, Leu248, Ala180, Ala250, Asn101, Asn258, Ala317, Met259, Val181, Val351, Thr314	–

Table 3 (continued)

Compound	$\Delta G_{binding}$	Hydrogen bond interaction	Hydrophobic interaction	Cation–π interaction
7n	−9.23	–	Asn258, Val315, Met259, Lys352, Val238, Leu242, Leu255, Ala354, Cys241, Ala250, Ala316, Asn249, Lys254, Leu248	–
7o	−9.45	–	Asn249, Lys254, Ala250, Cys241, Ala354, Ala316, Val238, Leu255, Asn258, Leu248	–
7p	−9.77	–	Ala354, Ala316, Cys241, Asn249, Val238, Leu255, Leu248, Lys254, Asn258, Ala250, Val181, Met259, Lys352	–
7q	−9.29	Asn258	Ala317, Asn249, Lys254, Leu248, Ala250, Val238, Lys352, Cys241, Ala354, Leu255, Ala316, Met259, Val181	–
7r	−10.09	–	Leu242, Val238, Ala316, Lys352, Leu255, Cys241, Ala354, Ala250, Leu248, Lys254, Asn249, Met259, Val181, Asn258	–
7s	−10.44	–	Ala317, Cys241, Val238, Lys352, Ala316, Ala250, Ala354, Asn249, Leu248, Lys254, Leu255, Met259, Asn258, Val181	–
7t	−9.90	–	Lys254, Leu248, Leu242, Val238, Ala354, Lys352, Ala316, Cys241, Asn249, Ala250, Leu255, Met259, Asn258, Val181	–
Colchicine	−8.69	Cys241, Val181	Met259, Ala180, Val315, Lys352, Leu248, Leu255, Ala250, Asn258	–

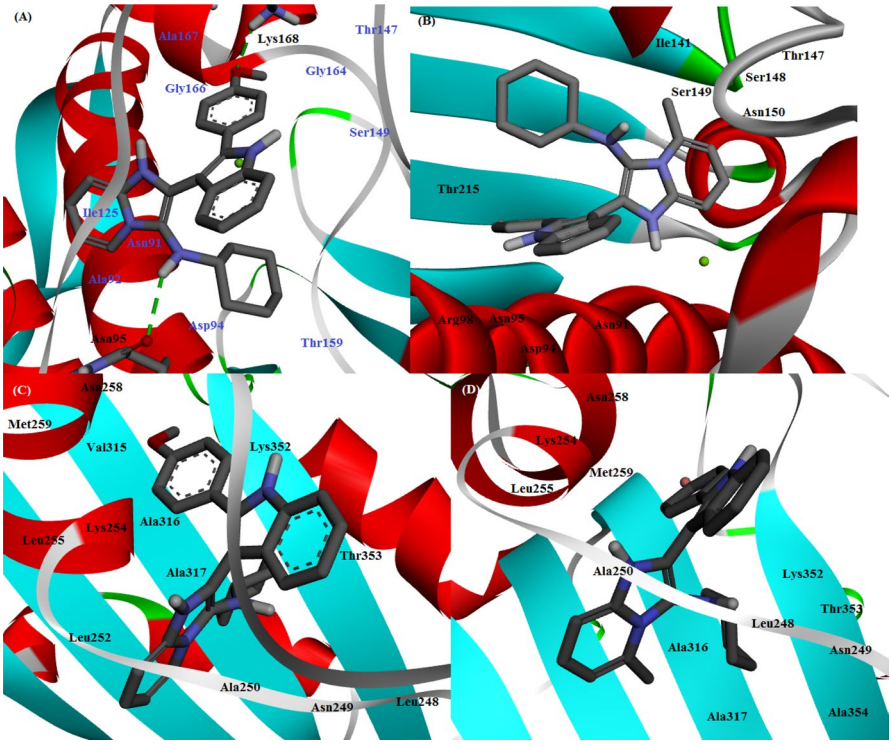

Fig. 5 Interactions of **7c** and **7j** in topoisomerase IIα (**a**, **b**) and in tubulin active sites (**c**, **d**)

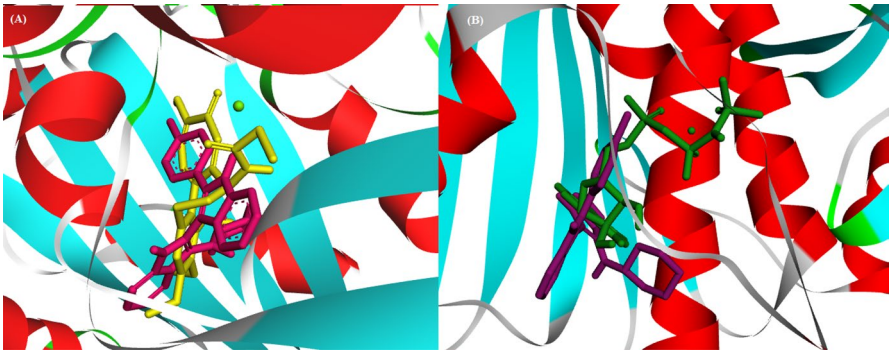

Fig. 6 Superimposition of **7f** and colchicine inside the tubulin active site (**a**), superimposition of **7f** and ANP inside the topoisomerase IIα active site (**b**)

topoisomerase IIα amino acids (Fig. 7). None of the studied compounds participated in cation–π stacking interactions with tubulin amino acids.

Molecular docking simulations showed that all compounds had more in silico affinity to tubulin compared to the topoisomerase IIα enzyme active site. This

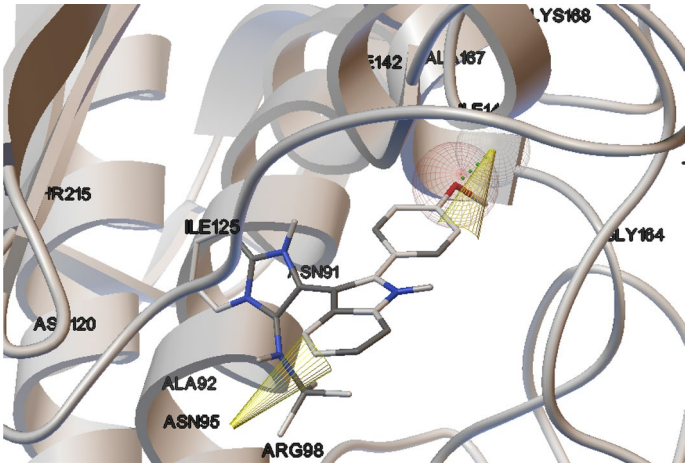

Fig. 7 Compound **7n** inside the topoisomerase IIα enzyme binding site. Orientations of **7n** phenyl ring, Arg98 guanidino and Lys168 amine groups in cation–π stacking interactions are demonstrated by *conical labels*

suggests that all the compounds might be stronger inhibitors of tubulin copmared with the topoisomerase IIα enzyme.

Conclusion

The present study describes the synthesis of a series of imidazopyridine derivatives of indole (**7a**–**t**). All the synthesized analogs were screened for antiproliferative activity against the A-594, Hep-G2, T-47D and MCF-7 cell lines using the MTT assay and with colchicine and etoposide as reference drugs. Structure–activity relationships analysis revealed that the presence of the cyclohexyl ring substituted to the second amine of the imidazopyridyl moiety, and that the phenyl ring (**7a**) and *para*-methylphenyl ring (**7f**) of the C-2 indole ring are appropriate for the cytotoxic activity against the A-594 cell line. In addition, compounds **7d** and **7j** with the *para*-chlorophenyl ring and the *para*-bromophenyl ring of the C-2 indole ring, respectively, showed the most potent activity against the Hep-G2 cell line. However, morphological analysis by the acridine orange/ethidium bromide double-staining test and flow cytometry analysis confirmed the induction of apoptosis in A-549 cells by compounds **7a** and **7f**. Molecular docking studies were performed to recognize the effects of substituents on the anticancer activity. Molecular docking studies established the binding modes of this series into tubulin and the ATPase domain of topoisomerase active sites, and also exposed the favorable interactions of the active molecules with the two enzyme residues. The higher $\Delta G_{\text{binding}}$ obtained for the compounds of the **7a**–**k** series compared with the $\Delta G_{\text{binding}}$ of the **7l**–**t** members confirmed the effect of the higher lipophilicity on hydrophobic interactions with the studied enzymes. Moreover, all the compounds showed a higher affinity to tubulin than to the topoisomerase IIα enzyme. Further investigations on these derivatives

could lead to more potent compounds as promising candidates for the development of new anticancer chemotherapy.

Acknowledgements This work was supported by grants from the Isfahan University of Medical Sciences and the Tehran University of Medical Sciences.

Compliance with ethical standards

Conflict of interest The authors declare that they have no conflict of interest.

References

1. H. Patel, N. Darji, J. Pillai, B. Patel, Int. J. Drug. Res. Tech. **2**, 225 (2012)
2. S. Shaaban, A. Negm, E.E. Ibrahim, A.A. Elrazak, Oncol. Rev. **8**, 246 (2014)
3. J.M. Yi, X.F. Zhang, X.J. Huan, S.S. Song, W. Wang, Q.T. Tian, Y.M. Sun, Y. Chen, J. Ding, Y.Q. Wang, C.H. Yang, Z.H. Miao, Oncotarget **6**, 8960 (2015)
4. K.E. Hevener, A.T. Verstak, K.E. Lutat, D.L. Riggsbee, J.W. Mooney, Acta Pharm. Sin. B **8**(6), 844 (2018)
5. D.S. Takur, Int. J. Pharm. Sci. Nanotechnol. **3**(4), 1173 (2011)
6. N. Fani, A.K. Bordbar, Y. Ghayeb, S. Sepehri, J. Biomol. Struct. Dyn. **33**(3), 471 (2015)
7. N. Fani, A.K. Bordbar, Y. Ghayeb, S. Sepehri, J. Biomol. Struct. Dyn. **33**(10), 2285 (2015)
8. A. Basnet, P. Thapa, R. Karki, H. Choi, J.H. Choi, M. Yun, B.S. Jeong, Y. Jahng, Y. Na, W.J. Cho, Y. Kwon, C.S. Lee, E.S. Lee, Bioorg. Med. Chem. Lett. **20**, 42 (2010)
9. S. Shaaban, F. Sasse, R. Diestel, B. Hinkelmann, Y. Muthukumar, R.P. Verma, C. Jacob, Eur. J. Med. Chem. **58**, 192 (2012)
10. S. Shaaban, A. Negm, A.M. Ashmawy, D.M. Ahmed, L.A. Wessjohann, Eur. J. Med. Chem. **122**, 55 (2016)
11. S. Shaaban, D. Vervandier-Fasseur, P. Andreoletti, A. Zarrouk, P. Richard, A. Negm, G. Manolikakes, C. Jacob, M. Cherkaoui-Malki, Bioorg. Chem. **80**, 43 (2018)
12. P.C. Diao, K.H. Hong, Q. Li, M.J. Hu, Y.F. Ma, W.W. You, P.L. Zhao, Eur. J. Med. Chem. **134**, 110 (2017)
13. D.R. Kerzare, P.B. Khedekar, J. Pharmsci. Biosci. Res. **6**(1), 144 (2016)
14. S. Suzan, Curr. Org. Chem. **21**(20), 2068 (2017)
15. A.M. Metwally, S. Shaaban, B.F. Abdel-Wahab, G.A. El-Hiti, Curr. Org. Chem. **13**(14), 1475 (2009)
16. S.N. Baytas, N. Inceler, A. Yılmaz, A. Olgac, S. Menevse, E. Hamel, R. Bortolozzi, G. Viola, Bioorg. Med. Chem. **22**, 3096 (2014)
17. J.P. Perchellet, E.M. Perchellet, C.R. Singh, Anticancer Res. **34**(4), 1643 (2014)
18. P. Chen, Y.X. Zhuang, P.C. Diao, F. Yang, S.Y. Wu, L. Lv, W.W. You, P.L. Zhao, Eur. J. Med. Chem. **162**, 525 (2019)
19. G.L. Regina, R. Bai, A. Coluccia, V. Famiglini, S. Pelliccia, S. Passacantilli, C. Mazzoccoli, V. Ruggieri, A. Verrico, A. Miele, L. Monti, M. Nalli, R. Alfonsi, L.D. Marcotullio, A. Gulino, B. Ricci, A. Soriani, A. Santoni, M. Caraglia, S. Porto, E.D. Pozzo, C. Martini, A. Brancale, L. Marinelli, E. Novellino, S. Vultaggio, M. Varasi, C. Mercurio, C. Bigogno, G.M. Dondio, E. Hamel, P. Lavia, R. Silvestri, J. Med. Chem. **58**(15), 5789 (2015)
20. A.V. Subba Rao, M.V. Vishnu Vardhan, N.V. Subba Reddy, T. Srinivasa Reddy, S.P. Shaik, C. Bagul, A. Kamal, Bioorg. Chem. **69**, 7 (2016)
21. T.S. Harrison, G.M. Keating, CNS Drugs **19**, 65 (2005)
22. S. Shaaban, B.F. Abdel-Wahab, Mol Divers. **20**(1), 233 (2016)
23. K. Okseon, J. Yujeong, H. Lee, S.S. Hong, S. Hong, J. Med. Chem. **54**, 2455 (2011)
24. A. Kamal, V.S. Reddy, S. Karnewar, S.S. Chourasiya, A.B. Shaik, G.B. Kumar, C. Kishor, M.K. Reddy, M.P. Narasimha Rao, A. Nagabhushana, K.V. Ramakrishna, A. Addlagatta, S. Kotamraju, Chem. Med. Chem. **8**(12), 2015 (2013)
25. A.T. Baviskar, C. Madaan, R. Preet, P. Mohapatra, V. Jain, A. Agarwal, S.K. Guchhait, C.N. Kundu, U.C. Banerjee, P.V. Bharatam, J. Med. Chem. **54**, 5013 (2011)

26. K.T. Ashitha, C.T.F. Salfeena, J. Renjitha, V.P. Kumar, R. Parveen, B.S. Sasidhar, Curr. Bioact. Compd. **14**(4), 445 (2018)
27. Z. Bakherad, M. Safavi, A. Fassihi, H. Sadeghi-Aliabadi, M. Bakherad, H. Rastegar, J.B. Ghasemi, S. Sepehri, L. Saghaie, M. Mahdavi, Res. Chem. Intermed. **45**(5), 2827 (2019)
28. M. Safavi, N. Esmati, S.K. Ardestani, S. Emami, S. Ajdari, J. Davoodi, A. Shafiee, A. Foroumadi, Eur. J. Med. Chem. **58**, 573 (2012)
29. S. Sepehri, S. Soleymani, R. Zabihollahi, M.R. Aghasadeghi, M. Sadat, L. Saghaie, A. Fassihi, Chem. Biodivers. **14**(12), e1700295 (2017)
30. T. Akbarzadeh, S. Noushini, S. Taban, M. Mahdavi, M. Khoshneviszadeh, M. Saeedi, Mol. Divers. **19**, 273 (2015)
31. M. Safavi, A. Ashtari, F. Khalili, S.S. Mirfazli, M. Saeedi, S. Ardestani, K.P. Ranjbar, R.M. Barazandeh Tehrani, B. Larijani, M. Mahdavi, Chem. Biol. Drug. Des. **92**(1), 1373 (2018)
32. S. Sepehri, L. Saghaie, A. Fassihi, Mol. Inform. **36**(3), 1 (2017)

Publisher's Note Springer Nature remains neutral with regard to jurisdictional claims in published maps and institutional affiliations.

Affiliations

Zohreh Bakherad[1,5] · Maliheh Safavi[2] · Saghi Sepehri[3] · Afshin Fassihi[1] · Hojjat Sadeghi-Aliabadi[1] · Mohammad Bakherad[4] · Hossein Rastegar[5] · Bagher Larijani[6] · Lotfollah Saghaie[1] · Mohammad Mahdavi[6]

✉ Lotfollah Saghaie
saghaie@pharm.mui.ac.ir

✉ Mohammad Mahdavi
momahdavi@tums.ac.ir

[1] Department of Medicinal Chemistry, School of Pharmacy and Pharmaceutical Sciences, Isfahan University of Medical Sciences, Isfahan 81746-73461, Iran

[2] Department of Biotechnology, Iranian Research Organization for Science and Technology, Tehran 33535-111, Iran

[3] Department of Medicinal Chemistry, School of Pharmacy, Ardabil University of Medical Sciences, Ardabil 5618953141, Iran

[4] School of Chemistry, Shahrood University of Technology, Shahrood, Iran

[5] Food and Drug Control Laboratories, Food and Drug Laboratory Research Center, MOE and ME, Tehran, Iran

[6] Endocrinology and Metabolism Research Center, Endocrinology and Metabolism Research Institute, Tehran University of Medical Sciences, Tehran, Iran